



Measurement of the differential cross section and charge asymmetry for inclusive $pp \rightarrow W^\pm + X$ production at $\sqrt{s} = 8$ TeV

CMS Collaboration*

CERN, 1211 Geneva 23, Switzerland

Received: 5 March 2016 / Accepted: 1 August 2016 / Published online: 22 August 2016

© CERN for the benefit of the CMS collaboration 2016. This article is published with open access at Springerlink.com

Abstract The differential cross section and charge asymmetry for inclusive $pp \rightarrow W^\pm + X \rightarrow \mu^\pm \nu + X$ production at $\sqrt{s} = 8$ TeV are measured as a function of muon pseudorapidity. The data sample corresponds to an integrated luminosity of 18.8 fb^{-1} recorded with the CMS detector at the LHC. These results provide important constraints on the parton distribution functions of the proton in the range of the Bjorken scaling variable x from 10^{-3} to 10^{-1} .

1 Introduction

We present measurements of the $pp \rightarrow W^\pm + X \rightarrow \mu^\pm \nu + X$ differential cross section and the muon charge asymmetry that provide important constraints on the valence and sea quark distributions in the proton. Uncertainties in the parton distribution functions (PDF) have become a limiting factor for the precision of many inclusive and differential cross section calculations, given the development of precise theoretical tools describing hard scattering processes in pp collisions.

For each charge of the W boson, the differential cross section,

$$\sigma_\eta^\pm = \frac{d\sigma}{d\eta}(pp \rightarrow W^\pm + X \rightarrow \mu^\pm \nu + X), \quad (1)$$

is measured in bins of muon pseudorapidity $\eta = -\ln \tan(\theta/2)$ in the laboratory frame, where θ is the polar angle of the muon direction with respect to the beam axis. Current theoretical calculations predict these cross sections with next-to-next-to-leading-order (NNLO) accuracy in perturbative quantum chromodynamics (QCD). The dominant W^\pm boson production occurs through the annihilation of a valence quark from one of the protons with a sea antiquark from the other: $u\bar{d} \rightarrow W^+$ and $d\bar{u} \rightarrow W^-$. Because of the presence of two valence u quarks in the proton, W^+ bosons are produced more often than W^- bosons. Precise measurement of the charge asymmetry as a function of the muon η ,

$$A(\eta) = \frac{\sigma_\eta^+ - \sigma_\eta^-}{\sigma_\eta^+ + \sigma_\eta^-}, \quad (2)$$

provides significant constraints on the ratio of u and d quark distributions in the proton for values of x , the Bjorken scaling variable [1], between 10^{-3} and 10^{-1} .

The W^\pm boson production asymmetry was previously studied in $p\bar{p}$ collisions by the CDF and D0 collaborations [2–6]. At the LHC, the first measurements of the lepton charge asymmetries were performed by the CMS, ATLAS, and LHCb experiments using data collected in 2010 [7–9]. The CMS experiment has further improved the measurement precision in both the electron and muon decay channels using data from pp collisions at $\sqrt{s} = 7$ TeV corresponding to integrated luminosities of 0.84 and 4.7 fb^{-1} in the electron [10] and muon [11] decay channels, respectively.

This measurement is based on a data sample of pp collisions at $\sqrt{s} = 8$ TeV collected by CMS during 2012, corresponding to an integrated luminosity of 18.8 fb^{-1} . At $\sqrt{s} = 8$ TeV the average value of the Bjorken scaling variable for the interacting partons in W^\pm boson production is lower than at $\sqrt{s} = 7$ TeV, which is expected to result in a lower W^\pm boson production charge asymmetry. This measurement provides important constraints on the proton PDFs, which is illustrated by the QCD analysis also presented in this paper.

2 CMS detector

The central feature of the CMS apparatus is a superconducting solenoid of 6 m internal diameter, providing a magnetic field of 3.8 T. Within the solenoid volume are a silicon pixel and strip tracker, a lead tungstate crystal electromagnetic calorimeter, and a brass and scintillator hadron calorimeter, each composed of a barrel and two endcap sections. Muons are measured in gas-ionization detectors embedded in the steel flux-return yoke outside the solenoid. Extensive forward calorimetry complements the coverage provided by the

*e-mail: cms-publication-committee-chair@cern.ch

barrel and endcap detectors. A more detailed description of the CMS detector can be found in Ref. [12].

3 Data selection and simulation

A $W^\pm \rightarrow \mu^\pm \nu$ event is characterized by an isolated muon with a high transverse momentum p_T and a large missing transverse energy E_T associated with an undetected neutrino. Events in this sample are collected with an isolated single-muon trigger with a p_T threshold of 24 GeV. To reduce the background, identification and isolation criteria are applied to the reconstructed muons. These requirements are similar to those used in the previous measurement [11]. Muon tracks must be reconstructed in both the silicon tracker and the muon detectors. The global muon fit is required to have a χ^2 per degree of freedom less than 10. The pseudorapidity coverage for reconstructed muons is restricted to $|\eta| < 2.4$. Cosmic ray contamination is largely reduced by rejecting the muon candidates with a large (> 0.2 cm) distance of closest approach to the primary vertex in the transverse plane. The isolation criterion is based on additional tracks reconstructed in a cone of $\sqrt{(\Delta\eta)^2 + (\Delta\phi)^2} < 0.3$ around the muon, where ϕ is the azimuthal angle (in radians) in the laboratory frame. The muon candidate is rejected if the scalar p_T sum of these tracks is more than 10 % of the muon p_T . The selected muon candidate with the largest p_T , identified as a signal muon from the W boson decay, is required to have a $p_T > 25$ GeV and also to be the particle that triggered the event. To reduce the background from Drell–Yan (DY) dimuon production, events containing a second identified muon with $p_T > 15$ GeV are rejected.

A total of about 61 million $W^+ \rightarrow \mu^+ \nu$ and 45 million $W^- \rightarrow \mu^- \bar{\nu}$ candidate events are selected. The $W^\pm \rightarrow \mu^\pm \nu$ signal is contaminated with backgrounds that also produce a muon with high p_T . The major background sources are (i) multijet (QCD) events with high- p_T muons produced in hadron decays (about 10 % of the selected sample), and (ii) $Z/\gamma^* \rightarrow \mu^+ \mu^-$ events (5 % of the sample). The contribution from other backgrounds, such as $W^\pm \rightarrow \tau^\pm \nu$ (2.6 %), $Z/\gamma^* \rightarrow \tau^+ \tau^-$ (0.5 %), and $t\bar{t}$ (0.5 %) events, is relatively small. The contributions from single top quark (0.14 %) and diboson (0.07 %) events, as well as from cosmic muons (10^{-5}), are negligible.

Simulated samples are used to model the signal and background processes. The signal, as well as the electroweak and $t\bar{t}$ background samples, is based on the next-to-leading-order (NLO) matrix element calculations implemented in the POWHEG Monte Carlo (MC) event generator [13–16], interfaced with PYTHIA6 [17] for parton showering and hadronization, including electromagnetic final-state radiation (FSR). The CT10 NLO PDFs [18] are used. The τ lepton decays in relevant processes are simulated with TAUOLA [19]. The

QCD background is generated with PYTHIA6 using CTEQ6L PDF [20].

The MC events are overlaid by simulated minimum-bias events to model additional pp interactions (pileup) present in data. The detector response to all generated particles is simulated with GEANT4 [21]. Final-state particles are reconstructed with the same algorithms used for the data sample.

4 Corrections to the data and simulations

The fiducial cross sections are measured for muon $p_T > 25$ GeV in 11 bins of absolute pseudorapidity, covering the range $|\eta| < 2.4$. The $|\eta|$ binning is such that the migration effects due to the finite η resolution are negligible. In each $|\eta|$ bin, the number of $W^+ \rightarrow \mu^+ \nu$ and $W^- \rightarrow \mu^- \nu$ events is extracted by fitting the E_T distributions with signal and background distributions (templates). The template shapes and initial normalizations are derived from MC simulations. To improve the simulation, several corrections are applied to the MC samples. The corrections, which are similar to those used in the previous measurement [11], are briefly summarized below.

All simulated events are weighted to match the pileup distribution in data. The weight factors are based on the measured instantaneous luminosity and minimum-bias cross section leading to a good description of the average number of reconstructed vertices in the data.

Accurate calibration of the muon momentum is important for the proper modeling of the yields of W^\pm events and of the shapes of E_T templates. Dominant sources of the muon momentum mismeasurement are the mismodeling of the tracker alignment and the magnetic field. Muon momentum correction factors are derived using $Z/\gamma^* \rightarrow \mu^+ \mu^-$ events in several iterations [22]. First, “reference” distributions are defined based on the MC generated muons, with momenta smeared by the reconstruction resolution. Then, corrections to muon momentum in bins of η and ϕ are extracted separately for positively and negatively charged muons. These corrections match the mean values of reconstructed $1/p_T$ spectra to the corresponding reference values. Finally, correction factors are tuned further by comparing the reconstructed dimuon invariant mass spectra in each μ^+ and μ^- pseudorapidity bin with the reference. The correction factors are determined separately for data and simulated events following the same procedure.

The overall muon selection efficiency includes contributions from reconstruction, identification, isolation, and trigger efficiencies. Each component is measured from $Z/\gamma^* \rightarrow \mu^+ \mu^-$ events using the “tag-and-probe” method [23, 24]. The efficiencies are measured in bins of η and p_T for μ^+ and μ^- separately. Each η bin of the efficiency measurement is fully contained in a single $|\eta|$ bin used for the asymmetry

measurement. The total average efficiency is about 85 % at central rapidities and drops to about 50 % in the last $|\eta|$ bin. The ratio of the average μ^+ and μ^- efficiencies varies within 0.6 % of unity in the first 10 $|\eta|$ bins. In the last bin the ratio is 0.98. The same procedure is used in data and MC simulation, and scale factors are determined to match the MC simulation efficiencies to data.

Template shapes, used in the fits, are based on the missing transverse momentum (\vec{p}_T^{miss}) reconstructed with the particle-flow algorithm [25, 26]. The \vec{p}_T^{miss} is defined as the projection on the plane perpendicular to the beams of the negative vector sum of the momenta of all reconstructed particles in an event. A set of corrections is applied to \vec{p}_T^{miss} in order to improve the modeling of distributions of $E_T = |\vec{p}_T^{\text{miss}}|$ in data and MC templates. First, the average bias in the \vec{p}_T^{miss} -component along the direction of \vec{p}_T -sum of charged particles associated with the pileup vertices is removed [27]. Second, the muon momentum correction to \vec{p}_T , described above, is added vectorially to \vec{p}_T^{miss} . In addition, the “ ϕ -modulation” corrections, which increase linearly as a function of pileup, make the $\phi(\vec{p}_T^{\text{miss}})$ distributions uniform [27]. The above corrections are applied to both data and simulated events. The final set of corrections, derived from the “hadronic recoil” technique [28, 29], is applied to simulated $W^\pm \rightarrow \mu^\pm \nu$, $Z/\gamma^* \rightarrow \mu^+ \mu^-$, and QCD events to match the average \vec{p}_T^{miss} scale and resolution to data.

The modeling of the multijet events is further improved with a set of corrections derived from a QCD control sample selected by inverting the offline isolation requirement for events collected using a prescaled muon trigger with no isolation requirement. Muon p_T -dependent weight factors are determined for the QCD simulation that match the muon p_T distributions with data. The QCD control sample is also used to derive ratios between the yields with positive and negative muons in each muon $|\eta|$ bin. These ratios are used to constrain the relative QCD contributions to W^+ and W^- events, as described in Sect. 5.

5 Signal extraction

In each of the 11 muon $|\eta|$ bins, yields of W^+ and W^- events are obtained from the simultaneous χ^2 -fit of the E_T distributions of μ^+ and μ^- events. The definition of χ^2 used in the fit takes into account the statistical uncertainties in the simulated templates. The shapes of the E_T distributions for the $W^\pm \rightarrow \mu^\pm \nu$ signal and the backgrounds are taken from the MC simulation after correcting for mismodeling of the detector response and for the p_T distribution of W bosons. All electroweak and $t\bar{t}$ background samples are normalized to the integrated luminosity using the theoretical cross sections calculated at NNLO. Each simulated event is also weighted with scale factors to match the average muon selection efficiencies in data. In addition, mass-dependent correction factors are applied to $Z/\gamma^* \rightarrow \mu^+ \mu^-$ simulated events to match the observed mass distribution of dimuon events in data.

The W^+ and W^- signal yields and the total QCD background normalization are free parameters in each fit. The relative contributions of QCD background events in the W^+ and W^- samples are constrained to values obtained from the QCD control sample. The $W^\pm \rightarrow \tau^\pm \nu$ background is normalized to the $W^\pm \rightarrow \mu^\pm \nu$ signal, for each charge, using the scale factors corresponding to the free parameters of the signal yield. The normalizations of the remaining electroweak and $t\bar{t}$ backgrounds are fixed in the fit.

Table 1 summarizes the fitted yields of W^+ (N^+) and W^- (N^-) events, the correlation coefficient ($\rho_{+,-}$), and the χ^2 value for each fit. Examples of fits for three $|\eta|$ ranges are shown in Fig. 1. The ratio of the data to the final fit, shown below each distribution, demonstrates good agreement of the fits with data. It should be noted that the χ^2 values reported in Table 1 are calculated using the statistical uncertainties of both data and simulated templates; systematic uncertainties are not taken into account.

For each muon charge and $|\eta|$ bin, the fiducial cross section is calculated as

Table 1 Summary of the fitted N^+ , N^- , the correlation ($\rho_{+,-}$) between the uncertainties in N^+ and N^- , and the χ^2 of the fit for each $|\eta|$ bin. The number of degrees of freedom (n_{dof}) in each fit is 197. The quoted uncertainties are statistical and include statistical uncertainties in the templates. The correlation coefficients are expressed as percentages

$ \eta $ bin	χ^2 ($n_{\text{dof}} = 197$)	N^+ (10^3)	N^- (10^3)	$\rho_{+,-}$ (%)
0.00–0.20	238	4648.5 ± 4.2	3584.9 ± 3.8	18.9
0.20–0.40	242	4414.5 ± 4.0	3360.9 ± 3.7	18.8
0.40–0.60	248	4893.8 ± 4.3	3692.5 ± 3.9	18.9
0.60–0.80	199	4900.1 ± 4.3	3621.3 ± 3.8	19.2
0.80–1.00	218	4420.8 ± 4.0	3218.0 ± 3.6	18.7
1.00–1.20	204	4235.7 ± 3.9	2949.2 ± 3.4	18.5
1.20–1.40	193	4176.8 ± 3.9	2827.0 ± 3.5	19.3
1.40–1.60	213	4351.2 ± 4.2	2864.7 ± 3.7	19.3
1.60–1.85	208	4956.2 ± 4.4	3134.1 ± 3.9	19.5
1.85–2.10	238	5292.9 ± 4.4	3229.6 ± 3.8	18.5
2.10–2.40	229	4023.7 ± 3.9	2428.2 ± 3.3	17.6

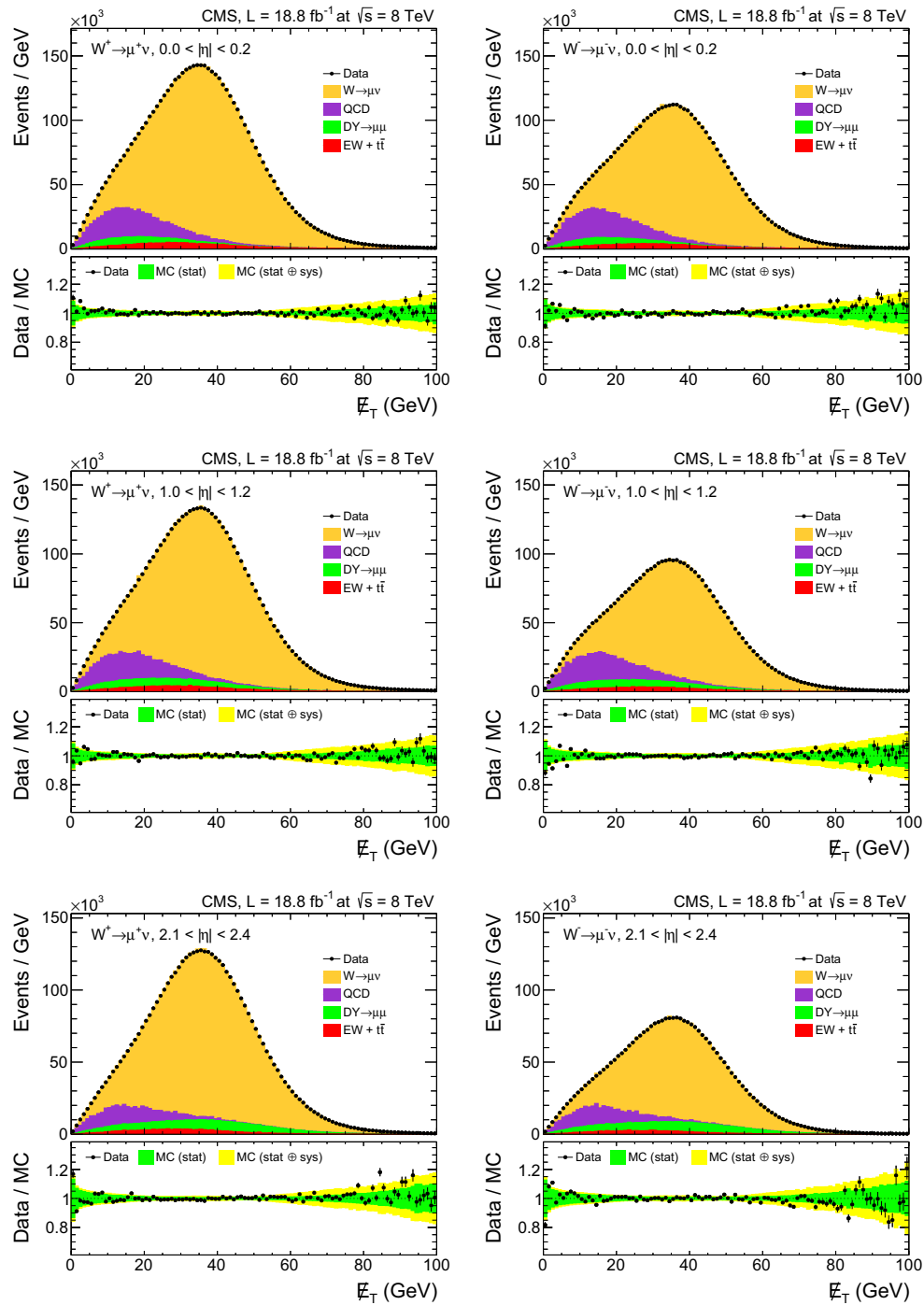


Fig. 1 Examples of fits in three $|\eta|$ ranges: $0.0 < |\eta| < 0.2$ (top), $1.0 < |\eta| < 1.2$ (center), and $2.1 < |\eta| < 2.4$ (bottom). For each η range, results for W^+ (left) and W^- (right) are shown. The ratios between the data points and the final fits are shown at the bottom of each panel

$$\sigma_{\eta}^{\pm} = \frac{1}{2\Delta\eta} \frac{N^{\pm}}{\epsilon^{\pm} \epsilon_{\text{FSR}}^{\pm} \mathcal{L}_{\text{int}}}, \quad (3)$$

where ϵ^{\pm} is the average μ^{\pm} selection efficiency per $|\eta|$ bin, ϵ_{FSR} takes into account the event loss within the muon p_T

acceptance due to the final-state photon emission, and \mathcal{L}_{int} is the integrated luminosity of the data sample. Each $\epsilon_{\text{FSR}}^{\pm}$ factor, defined as a ratio of the numbers of events within the p_T acceptance after and before FSR, is evaluated using the signal MC samples.

6 Systematic uncertainties

To estimate the systematic uncertainties in the muon selection efficiencies, several variations are applied to the measured efficiency tables. First, the efficiency values in each η - p_T bin are varied within their statistical errors for data and simulation independently. In each pseudo-experiment the varied set of efficiencies is used to correct the MC simulation templates and extract the cross sections using Eq. (3). The standard deviation of the resulting distribution is taken as a systematic uncertainty for each charge and $|\eta|$ bin. The statistical uncertainties between the two charges and all η - p_T bins are uncorrelated. Second, the offline muon selection efficiency scale factors are varied by $\pm 0.5\%$ coherently for both charges and all bins. The trigger selection efficiency scale factors are varied by $\pm 0.2\%$, assuming no correlations between the η bins, but $+100\%$ correlations between the charges and p_T bins. The above systematic variations take into account uncertainties associated with the tag-and-probe technique and are assessed by varying signal and background dimuon mass shapes, levels of background, and dimuon mass range and binning used in the fits. Finally, an additional $\pm 100\%$ correlated variation is applied based on the bin-by-bin difference between the true and measured efficiencies in the $Z/\gamma^* \rightarrow \mu^+\mu^-$ MC sample. This difference changes gradually from about 0.5% in the first bin to about -2% in the last bin. This contribution is the main source of negative correlations in the systematic uncertainties between the central and high rapidity bins. The total systematic uncertainty in the efficiency is obtained by adding up the four covariance matrices corresponding to the above variations.

A possible mismeasurement of the charge of the muon could lead to a bias in the observed asymmetry between the W^+ and W^- event rates. The muon charge misidentification rate has been studied in detail and was found to be negligible (10^{-5}) [7].

The muon momentum correction affects the yields and the shapes of the E_T distributions in both data and MC simulation. To estimate the systematic uncertainty, the muon correction parameters in each η - ϕ bin and overall scale are varied within their uncertainties. The standard deviation of the resulting cross section distribution for each charge and muon $|\eta|$ bin is taken as the systematic uncertainty and the corresponding correlations are calculated. Finite detector resolution effects, which result in the migration of events around the p_T threshold and between $|\eta|$ bins, have been studied with the signal MC sample and found to have a negligible impact on the measured cross sections and asymmetries.

There are two sources of systematic uncertainties associated with the QCD background estimate. One is the uncertainty in the ratio of QCD background events in the W^+ and W^- samples (R_{\pm}^{QCD}). Whereas the total QCD normalization is one of the free parameters in the fit, R_{\pm}^{QCD} is constrained to

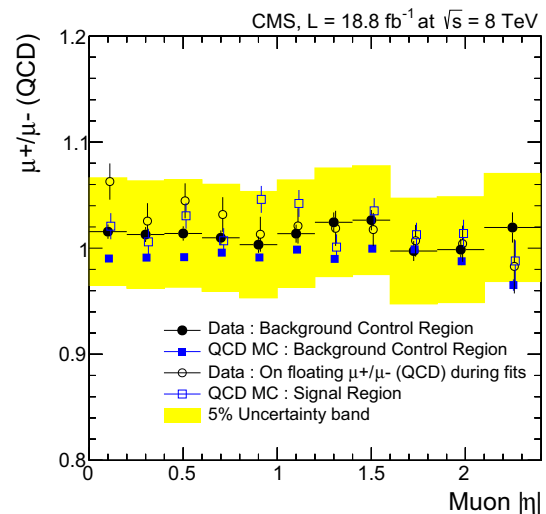


Fig. 2 Distribution of R_{\pm}^{QCD} in QCD control region for data (solid circles), QCD control region for simulation (solid squares), and signal region for simulation (open squares). Open circles show the R_{\pm}^{QCD} distribution when QCD contributions in W^+ and W^- events are not constrained. Shaded area indicates assigned systematic uncertainty

the value observed in the QCD control sample, which varies within 3% of unity depending on the $|\eta|$ bin. The corresponding systematic uncertainty is evaluated by changing it by $\pm 5\%$ in each $|\eta|$ bin. This variation covers the maximum deviations indicated by the QCD MC simulation, as indicated in Fig. 2. The resulting systematic uncertainties are assumed to be uncorrelated between the $|\eta|$ bins. Additionally, to take into account possible bias in this ratio due to different flavor composition in the signal and QCD control regions, the average difference of this ratio between the signal and QCD control regions is evaluated using the QCD MC simulation. This difference of about 3% is taken as an additional 100% -correlated systematic uncertainty in R_{\pm}^{QCD} . As a check, using the same shape for the QCD background in μ^+ and μ^- events, its normalization is allowed to float independently for the two charges. The resulting values of R_{\pm}^{QCD} are covered by the above systematic uncertainties.

The other component of systematic uncertainty, associated with the QCD background, is the E_T shape. To estimate the systematic uncertainty in modeling the shape of the E_T distributions in QCD events, additional fits are performed using the E_T distributions without the hadronic recoil corrections and the p_T -dependent scale factors; this results in a variation of about 2% in the average E_T resolution. The resulting shifts in the extracted cross section values in each $|\eta|$ bin are taken as systematic uncertainties. The correlations between the $|\eta|$ bins and the two charges are assumed to be 100% .

The normalization of the $Z/\gamma^* \rightarrow \mu^+\mu^-$ background in the signal region is corrected with mass-dependent scale

factors that match the dimuon mass distribution in MC simulation with data. The systematic uncertainty is the difference between the cross sections calculated with and without applying these corrections to the DY background normalizations. An uncertainty of 7 % is assigned to the $t\bar{t}$ theoretical cross section [30], which is used to normalize the $t\bar{t}$ background to the integrated luminosity of the data sample. In the fits, the $W^\pm \rightarrow \tau^\pm \nu$ background is normalized to the $W^\pm \rightarrow \mu^\pm \nu$ yields in data with a ratio obtained from the simulation. A ± 2 % uncertainty is assigned to the $W^\pm \rightarrow \tau^\pm \nu$ to $W^\pm \rightarrow \mu^\pm \nu$ ratio [31]. Each of the above variations is assumed to be fully correlated for the different bins and the two charges.

There are several sources of systematic uncertainty that affect the E_T shapes. The systematic uncertainty associated with the ϕ modulation of \vec{p}_T^{miss} is small and is evaluated by removing the corresponding correction to \vec{p}_T^{miss} . A 5 % uncertainty is assigned to the minimum bias cross section used to calculate the expected pileup distribution in data. To improve the agreement between data and simulation, the W boson p_T spectrum is weighted using factors determined by the ratios of the p_T distributions in $Z/\gamma^* \rightarrow \mu^+ \mu^-$ events in data and MC simulation. The difference in measured cross sections with and without this correction is taken as a systematic uncertainty. Each of the sources above are assumed to be fully correlated between the two charges and different bins. Systematic uncertainties associated with the recoil corrections are evaluated by varying the average recoil and resolution parameters within their uncertainties. The standard deviation of the resulting cross section distribution is taken as the systematic uncertainty and correlations between the two charges and different bins are calculated.

The emission of FSR photons tends, on average, to reduce the muon p_T . The observed post-FSR cross sections within the p_T acceptance are corrected using the $\epsilon_{\text{FSR}}^\pm$ factors derived from the signal MC sample. The difference between the p_T spectra of positive and negative muons results in smaller charge asymmetries after FSR compared with those before FSR within the same $p_T > 25$ GeV acceptance. These differences, which vary between 0.07 and 0.11 % depending on the $|\eta|$ bin, are corrected by the charge-dependent $\epsilon_{\text{FSR}}^\pm$ efficiency factors. The systematic uncertainty in the FSR modeling is estimated by reweighting events with radiated photons with correction factors that account for missing electroweak corrections in the parton shower [32,33]. The $\epsilon_{\text{FSR}}^\pm$ correction factors are reevaluated after such reweighting, and the difference between the cross sections, calculated with the new and default $\epsilon_{\text{FSR}}^\pm$ values, is taken as a systematic uncertainty. The correlations between the two charges and different $|\eta|$ bins are assumed to be 100 %. The effects of migration between the $|\eta|$ bins due to final-state photon emission have been evaluated with the signal MC sample and are found to be negligible.

The PDF uncertainties are evaluated by using the NLO MSTW2008 [34], CT10 [18], and NNPDF2.1 [35] PDF sets. All simulated events are weighted according to a given PDF set, varying both the template normalizations and shapes. For CT10 and MSTW2008 PDFs, asymmetric master equations are used [18,34]. For the NNPDF2.1 PDF set, the standard deviation of the extracted cross section distributions is taken as a systematic uncertainty. For the CT10, the 90 % confidence level (CL) uncertainty is rescaled to 68 % CL using a factor of 1.645. The half-width of the total envelope of all three PDF uncertainty bands is taken as the PDF uncertainty. The CT10 error set is used to estimate the correlations between the two charges and different $|\eta|$ bins.

Finally, a ± 2.6 % uncertainty [36] is assigned to the integrated luminosity of the data sample. The luminosity uncertainty is fully correlated between the $|\eta|$ bins and two charges. Therefore, this uncertainty cancels in the measured charge asymmetries. The uncertainty in the normalization of the electroweak backgrounds due to the luminosity uncertainty has a negligible impact on the measurements.

Table 2 summarizes the systematic uncertainties in the measured cross sections and asymmetries. For comparison, the statistical and luminosity uncertainties are also shown. The uncertainty in the integrated luminosity dominates the total uncertainties in the measured cross sections, while the uncertainty in the QCD background estimation dominates the uncertainties in the charge asymmetries. The uncertainties for the muon charge asymmetries are calculated from those in the differential cross sections, taking into account the correlations between the two charges.

The correlations in the systematic uncertainty between the charges and different $|\eta|$ bins are shown in Table 3. The full 22×22 correlation matrix C is split into four 11×11 blocks as

$$C = \begin{bmatrix} C_{++} & C_{+-} \\ C_{+-}^T & C_{--} \end{bmatrix}, \quad (4)$$

where the C_{++} and C_{--} matrices represent the bin-to-bin correlations of systematic uncertainties in σ_η^+ and σ_η^- , respectively, and C_{+-} describes the correlations between the two charges. To construct the total covariance matrix, the covariance matrix of the systematic uncertainties should be added to those of the statistical and integrated luminosity uncertainties. The latter are fully correlated between the two charges and $|\eta|$ bins. For the statistical uncertainties bin-to-bin correlations are zero; the correlations between the two charges are shown in Table 1.

7 Results

The measured cross sections and charge asymmetries are summarized in Table 4 and displayed in Fig. 3. The error bars

Table 2 Systematic uncertainties in cross sections ($\delta\sigma_{\eta}^{\pm}$) and charge asymmetry ($\delta\mathcal{A}$) for each $|\eta|$ bin. The statistical and integrated luminosity uncertainties are also shown for comparison. A detailed description of each systematic uncertainty is given in the text

$ \eta $ bin	0.0–0.2	0.2–0.4	0.4–0.6	0.6–0.8	0.8–1.0	1.0–1.2	1.2–1.4	1.4–1.6	1.6–1.85	1.85–2.1	2.1–2.4
$\delta\sigma_{\eta}^{+}$ (pb)											
Efficiency	5.5	7.0	6.3	6.2	6.6	4.5	4.3	4.3	5.3	6.9	17.7
Muon scale	0.4	0.4	0.4	0.4	0.4	0.5	0.5	0.5	0.5	0.5	0.4
QCD $+/-$	1.1	1.1	1.1	1.1	1.1	1.1	1.2	1.3	1.2	1.0	0.7
QCD shape	2.0	1.9	2.0	2.0	1.9	1.9	2.0	2.3	2.1	1.5	1.0
EW+t \bar{t} bkg	0.6	0.6	0.6	0.6	0.6	0.7	0.8	0.9	1.0	1.2	1.3
E_T shape	2.4	2.4	2.5	2.4	2.4	2.5	2.8	2.9	2.9	2.4	1.9
PDF	0.6	0.5	0.5	0.5	0.7	0.9	1.1	1.3	1.6	1.8	2.0
FSR	0.2	0.2	0.2	0.2	0.2	0.2	0.2	0.1	0.1	0.0	0.0
Total syst.	6.5	7.7	7.2	7.1	7.4	5.8	5.8	6.1	6.8	7.9	18.0
Int. lum.	19.3	19.5	19.5	19.6	19.8	19.9	20.1	20.1	20.2	20.0	19.5
Stat.	0.7	0.7	0.7	0.7	0.7	0.7	0.7	0.7	0.7	0.6	0.7
Total unc.	20.4	21.0	20.8	20.9	21.2	20.7	21.0	21.0	21.3	21.6	26.5
$\delta\sigma_{\eta}^{-}$ (pb)											
Efficiency	4.3	5.5	4.8	4.6	4.4	3.2	2.9	2.8	3.4	4.0	10.1
Muon scale	0.3	0.3	0.3	0.3	0.3	0.3	0.3	0.4	0.4	0.3	0.3
QCD $+/-$	0.9	0.9	0.9	0.9	0.9	0.9	1.0	1.0	1.0	0.8	0.5
QCD shape	1.8	1.8	1.9	1.8	1.8	1.8	2.0	2.1	2.1	1.5	1.0
EW+t \bar{t} bkg	0.5	0.5	0.5	0.6	0.6	0.6	0.7	0.8	0.9	1.1	1.2
E_T shape	2.2	2.2	2.3	2.2	2.3	2.4	2.5	2.8	2.7	2.3	1.7
PDF	0.6	0.6	0.5	0.5	0.7	0.8	1.1	1.2	1.5	1.6	1.9
FSR	0.2	0.2	0.1	0.1	0.1	0.1	0.1	0.1	0.1	0.1	0.1
Total syst.	5.3	6.4	5.7	5.5	5.5	4.6	4.6	4.9	5.2	5.3	10.6
Int. lum.	14.8	14.8	14.7	14.5	14.3	13.9	13.6	13.2	12.7	12.1	11.4
Stat.	0.6	0.6	0.6	0.6	0.6	0.6	0.6	0.6	0.6	0.6	0.6
Total unc.	15.7	16.1	15.8	15.5	15.3	14.7	14.3	14.1	13.7	13.2	15.6
$\delta\mathcal{A} \times 100$											
Efficiency	0.06	0.07	0.06	0.06	0.09	0.09	0.10	0.09	0.09	0.08	0.14
Muon scale	0.03	0.03	0.03	0.03	0.03	0.03	0.03	0.04	0.04	0.03	0.03
QCD $+/-$	0.15	0.15	0.15	0.15	0.15	0.15	0.16	0.18	0.17	0.14	0.10
QCD shape	0.02	0.03	0.03	0.03	0.04	0.04	0.05	0.06	0.07	0.05	0.04
EW+t \bar{t} bkg	0.03	0.03	0.03	0.03	0.03	0.03	0.03	0.03	0.04	0.04	0.05
E_T shape	0.03	0.04	0.04	0.04	0.05	0.06	0.06	0.09	0.09	0.09	0.07
PDF	0.03	0.02	0.02	0.02	0.02	0.03	0.04	0.05	0.05	0.09	0.08
FSR	0.00	0.00	0.00	0.00	0.00	0.00	0.00	0.00	0.00	0.00	0.01
Total syst.	0.17	0.18	0.18	0.18	0.19	0.20	0.22	0.23	0.23	0.22	0.21
Stat.	0.06	0.06	0.06	0.06	0.06	0.07	0.07	0.07	0.06	0.06	0.07
Total unc.	0.18	0.19	0.19	0.19	0.20	0.21	0.23	0.24	0.24	0.23	0.22

of the measurements represent both statistical and systematic uncertainties, including the uncertainty in the integrated luminosity. The measurements are compared with theoretical predictions based on several PDF sets. The predictions are obtained using the FEWZ 3.1 [37] NNLO MC calculation interfaced with CT10 [18], NNPDF3.0 [38], HERAPDF1.5

[39], MMHT2014 [40], and ABM12 [41] PDF sets. No electroweak corrections are included in these calculations. The error bars of the theoretical predictions represent the PDF uncertainty, which is the dominant source of uncertainty in these calculations. For the CT10, MMHT, HERA, and ABM PDFs, the uncertainties are calculated with their eigenvec-

Table 3 Correlation matrices of systematic uncertainties for σ_{η}^{\pm} and \mathcal{A} . The statistical and integrated luminosity uncertainties are not included. The full 22×22 correlation matrix for σ_{η}^{\pm} is presented as four blocks of 11×11 matrices, as shown in Eq. (4). The C_{++} and C_{--} blocks on the

diagonal represent the bin-to-bin correlations of $\delta\sigma_{\eta}^{+}$ and $\delta\sigma_{\eta}^{-}$, respectively. The off-diagonal C_{+-} and C_{+}^T blocks describe the correlations between the two charges. The values are expressed as percentages

$ \eta $ bin	0.0–0.2	0.2–0.4	0.4–0.6	0.6–0.8	0.8–1.0	1.0–1.2	1.2–1.4	1.4–1.6	1.6–1.85	1.85–2.1	2.1–2.4
Correlation matrix of systematic uncertainties in σ_{η}^{\pm}											
C_{++}											
0.00–0.20	100.0	90.3	91.3	91.2	90.2	81.8	69.4	63.3	32.9	6.1	–37.2
0.20–0.40		100.0	92.5	92.4	92.2	74.9	58.6	51.1	16.2	–11.8	–54.7
0.40–0.60			100.0	92.5	92.1	79.2	64.8	57.9	25.0	–2.8	–46.6
0.60–0.80				100.0	92.2	79.5	65.4	58.6	25.8	–1.9	–46.0
0.80–1.00					100.0	78.3	63.7	56.7	23.2	–4.5	–48.7
1.00–1.20						100.0	82.8	79.9	60.0	38.5	–3.9
1.20–1.40							100.0	85.6	74.8	58.4	20.5
1.40–1.60								100.0	79.8	65.6	30.0
1.60–1.85									100.0	86.6	64.5
1.85–2.10										100.0	83.8
2.10–2.40											100.0
C_{--}											
0.00–0.20	100.0	91.1	92.1	91.9	91.2	81.8	64.8	65.6	38.5	19.0	–31.5
0.20–0.40		100.0	92.8	92.3	91.2	74.6	53.0	54.4	23.1	2.2	–48.8
0.40–0.60			100.0	92.8	92.1	80.1	61.2	62.5	33.3	12.8	–38.7
0.60–0.80				100.0	92.3	81.3	63.4	64.6	36.2	15.8	–35.9
0.80–1.00					100.0	82.5	65.4	66.8	39.0	18.6	–33.3
1.00–1.20						100.0	83.5	84.1	67.9	52.2	5.4
1.20–1.40							100.0	88.9	83.9	73.2	35.4
1.40–1.60								100.0	83.8	72.6	33.1
1.60–1.85									100.0	88.5	64.4
1.85–2.10										100.0	80.4
2.10–2.40											100.0
C_{+-}											
0.00–0.20	92.7	89.5	90.1	89.9	89.0	78.7	61.1	61.7	34.6	16.0	–32.9
0.20–0.40	88.9	94.4	90.7	90.1	88.8	71.2	49.0	50.1	18.8	–1.2	–50.5
0.40–0.60	90.0	91.7	93.6	90.9	89.9	76.0	55.9	56.9	27.4	7.6	–42.2
0.60–0.80	89.7	91.4	90.9	93.2	89.9	76.2	56.4	57.3	28.1	8.3	–41.6
0.80–1.00	88.8	91.3	90.5	90.4	92.0	74.9	54.6	55.7	25.9	5.9	–44.1
1.00–1.20	80.4	74.4	78.8	80.1	80.8	87.9	77.4	77.4	60.4	45.7	0.8
1.20–1.40	68.5	58.5	65.4	67.3	68.7	82.1	86.3	82.8	74.5	63.8	25.2
1.40–1.60	62.6	51.2	59.0	61.2	62.9	80.1	84.7	86.4	79.6	70.5	34.8
1.60–1.85	32.7	16.8	26.9	29.8	32.2	61.8	78.4	77.1	89.1	87.0	68.2
1.85–2.10	6.0	–11.4	–0.8	2.3	4.9	40.4	63.9	61.7	82.1	91.4	86.0
2.10–2.40	–36.9	–54.0	–44.2	–41.7	–39.3	–1.0	29.0	26.2	58.5	75.1	98.2
Correlation matrix of systematic uncertainties in \mathcal{A}											
0.00–0.20	100.0	27.2	27.4	26.8	24.8	26.7	24.3	27.0	26.1	25.0	19.7
0.20–0.40		100.0	27.8	27.2	24.5	27.3	24.1	28.9	27.8	28.1	22.5
0.40–0.60			100.0	28.3	27.4	28.6	27.0	29.9	29.5	28.0	21.4
0.60–0.80				100.0	29.3	29.0	29.1	30.6	30.9	28.7	22.2
0.80–1.00					100.0	29.7	32.8	32.0	33.0	28.4	20.7
1.00–1.20						100.0	31.2	33.6	34.3	31.9	25.4
1.20–1.40							100.0	34.2	36.8	30.6	25.1
1.40–1.60								100.0	39.1	37.4	31.0
1.60–1.85									100.0	38.6	33.3
1.85–2.10										100.0	42.0
2.10–2.40											100.0

tor sets using asymmetric master equations where applicable. For the NNPDF set the standard deviations over its 100 replicas are evaluated.

The numerical values of the predictions are also shown in Table 4. We note that the previous lepton charge asymmetries measured by CMS at $\sqrt{s} = 7$ TeV have been included in the global PDF fits for the NNPDF3.0, MMHT2014, and ABM12 PDFs. The measured cross sections and charge asymmetries are well described by all considered PDF sets within their corresponding uncertainties.

8 QCD analysis

The muon charge asymmetry measurements at 8 TeV presented here are used in a QCD analysis at NNLO together with the combined measurements of neutral- and charged-current cross sections of deep inelastic electron(positron)-proton scattering (DIS) at HERA [42]. The correlations of the experimental uncertainties for the muon charge asymmetry and for the inclusive DIS cross sections are taken into account. The theoretical predictions are calculated at NLO by using the MCFM 6.8 program [43,44], which is interfaced to APPLGRID 1.4.56 [45]. The NNLO corrections are obtained by using k -factors, defined as ratios of the predictions at NNLO to the ones at NLO, both calculated with the FEWZ 3.1 [37] program, using NNLO CT10 [18] PDFs.

Version 1.1.1 of the open-source QCD fit framework for PDF determination HERAFitter [46,47] is used with the partons evolved by using the Dokshitzer–Gribov–Lipatov–Altarelli–Parisi equations [48–53] at NNLO, as implemented in the QCDNUM 17-00/06 program [54].

The Thorne–Roberts [34,55] general mass variable flavor number scheme at NNLO is used for the treatment of heavy-quark contributions with heavy-quark masses $m_c = 1.43$ GeV and $m_b = 4.5$ GeV. The renormalization and factorization scales are set to Q , which denotes the four-momentum transfer in case of the DIS data and the mass of the W boson in case of the muon charge asymmetry, respectively.

The strong coupling constant is set to $\alpha_s(m_Z) = 0.118$. The Q^2 range of HERA data is restricted to $Q^2 \geq Q_{\min}^2 = 3.5$ GeV² to assure the applicability of perturbative QCD over the kinematic range of the fit.

The procedure for the determination of the PDFs follows the approach used in the analysis in Ref. [11]. The parametrised PDFs are the gluon distribution, xg , the valence quark distributions, xu_v , xd_v , and the u-type and d-type anti-quark distributions, $x\bar{U}$, $x\bar{D}$. At the initial scale of the QCD evolution $Q_0^2 = 1.9$ GeV², the PDFs are parametrized as:

$$xg(x) = A_g x^{B_g} (1-x)^{C_g} (1 + D_g x), \quad (5)$$

$$xu_v(x) = A_{u_v} x^{B_{u_v}} (1-x)^{C_{u_v}} (1 + E_{u_v} x^2), \quad (6)$$

$$xd_v(x) = A_{d_v} x^{B_{d_v}} (1-x)^{C_{d_v}}, \quad (7)$$

$$x\bar{U}(x) = A_{\bar{U}} x^{B_{\bar{U}}} (1-x)^{C_{\bar{U}}} (1 + E_{\bar{U}} x^2), \quad (8)$$

$$x\bar{D}(x) = A_{\bar{D}} x^{B_{\bar{D}}} (1-x)^{C_{\bar{D}}}, \quad (9)$$

with the relations $x\bar{U} = x\bar{u}$ and $x\bar{D} = x\bar{d} + x\bar{s}$ assumed.

The normalization parameters A_{u_v} , A_{d_v} , and A_g are determined by the QCD sum rules, the B parameter is responsible for small- x behavior of the PDFs, and the parameter C describes the shape of the distribution as $x \rightarrow 1$. Additional constraints $B_{\bar{U}} = B_{\bar{D}}$ and $A_{\bar{U}} = A_{\bar{D}}(1 - f_s)$ are imposed with f_s being the strangeness fraction, $f_s = \bar{s}/(\bar{d} + \bar{s})$, which is fixed to $f_s = 0.31 \pm 0.08$ as in Ref. [34], consistent with the determination of the strangeness fraction by using the CMS measurements of W + charm production [11]. The χ^2 definition in the QCD analysis follows that of Eq. (32) of [42] without the logarithmic term. The parameters in Eqs. (5)–(9) were selected by first fitting with all D and E parameters set to zero. The other parameters were then included in the fit one at a time independently. The improvement of the χ^2 of the fits was monitored and the procedure was stopped when no further improvement was observed. This led to a 13-parameter fit.

The PDF uncertainties are estimated according to the general approach of HERAPDF1.0 [56] in which the experimental, model, and parametrization uncertainties are taken into account. A tolerance criterion of $\Delta\chi^2 = 1$ is adopted for defining the experimental uncertainties that originate from the measurements included in the analysis.

Model uncertainties arise from the variations in the values assumed for the heavy-quark masses m_b , m_c with $4.25 \leq m_b \leq 4.75$ GeV, $1.37 \leq m_c \leq 1.49$ GeV, following Ref. [42], and the value of Q_{\min}^2 imposed on the HERA data, which is varied in the interval $2.5 \leq Q_{\min}^2 \leq 5.0$ GeV². The strangeness fraction f_s is varied by its uncertainty.

The parametrization uncertainty is estimated by extending the functional form of all parton densities with additional parameters. The uncertainty is constructed as an envelope built from the maximal differences between the PDFs resulting from all the parametrization variations and the central fit at each x value. The total PDF uncertainty is obtained by adding experimental, model, and parametrization uncertainties in quadrature. In the following, the quoted uncertainties correspond to 68 % CL.

The global and partial χ^2 values for the data sets used are listed in Table 5, illustrating the consistency among the data sets used. The somewhat high χ^2/n_{dof} values for the combined DIS data are very similar to those observed in Ref. [42], where they are investigated in detail.

In the kinematic range probed, the final combined HERA DIS data currently provide the most significant constraints on the valence distributions. By adding these muon charge asymmetry measurements, the constraints can be signifi-

Table 4 Summary of the measured differential cross sections σ_{η}^{\pm} (pb) and charge asymmetry \mathcal{A} . The first uncertainty is statistical, the second uncertainty is systematic, and the third is the integrated luminosity uncertainty. The theoretical predictions are obtained using the FEWZ 3.1 [37] NNLO MC tool interfaced with five different PDF sets

$ \eta $ bin	Measurement	Theory				
	(\pm stat \pm syst \pm lumi)	CT10	NNPDF3.0	MMHT2014	ABM12	HERAPDF1.5
σ_{η}^{+} (pb)						
0.00–0.20	$743.7 \pm 0.7 \pm 6.5 \pm 19.3$	$759.7^{+19.3}_{-25.1}$	740.5 ± 16.8	$750.8^{+13.2}_{-10.8}$	764.2 ± 9.3	$762.8^{+6.8}_{-7.8}$
0.20–0.40	$749.5 \pm 0.7 \pm 7.7 \pm 19.5$	$761.2^{+19.2}_{-24.9}$	740.8 ± 16.6	$751.8^{+13.1}_{-10.6}$	766.0 ± 9.6	$764.7^{+7.2}_{-7.8}$
0.40–0.60	$751.9 \pm 0.7 \pm 7.2 \pm 19.5$	$763.6^{+19.1}_{-24.6}$	743.5 ± 16.5	$754.0^{+13.0}_{-10.3}$	769.4 ± 9.7	$767.9^{+6.5}_{-6.6}$
0.60–0.80	$755.0 \pm 0.7 \pm 7.1 \pm 19.6$	$769.1^{+18.6}_{-23.8}$	746.9 ± 16.0	$759.0^{+13.1}_{-10.1}$	773.8 ± 9.4	$772.0^{+7.8}_{-7.2}$
0.80–1.00	$761.9 \pm 0.7 \pm 7.4 \pm 19.8$	$773.4^{+18.2}_{-22.8}$	750.7 ± 16.0	$763.6^{+13.0}_{-9.8}$	780.0 ± 9.9	$777.5^{+7.6}_{-6.4}$
1.00–1.20	$766.0 \pm 0.7 \pm 5.8 \pm 19.9$	$777.8^{+17.7}_{-22.1}$	756.5 ± 15.8	$769.2^{+12.8}_{-9.8}$	784.9 ± 9.7	$782.5^{+8.2}_{-6.8}$
1.20–1.40	$774.4 \pm 0.7 \pm 5.8 \pm 20.1$	$785.0^{+17.7}_{-21.5}$	760.9 ± 15.6	$775.5^{+13.1}_{-10.5}$	791.5 ± 9.9	$787.3^{+8.7}_{-6.8}$
1.40–1.60	$774.6 \pm 0.7 \pm 6.1 \pm 20.1$	$793.7^{+17.5}_{-20.8}$	768.5 ± 15.7	$784.0^{+13.3}_{-11.3}$	799.7 ± 10.2	$796.7^{+11.4}_{-9.5}$
1.60–1.85	$776.4 \pm 0.7 \pm 6.8 \pm 20.2$	$784.4^{+16.9}_{-19.5}$	761.3 ± 15.4	$778.5^{+13.5}_{-12.4}$	792.4 ± 10.3	$788.9^{+15.0}_{-11.5}$
1.85–2.10	$771.1 \pm 0.6 \pm 7.9 \pm 20.0$	$785.5^{+16.9}_{-18.8}$	762.2 ± 15.7	$780.3^{+14.0}_{-14.0}$	791.6 ± 10.2	$788.9^{+17.6}_{-11.4}$
2.10–2.40	$748.3 \pm 0.7 \pm 18.0 \pm 19.5$	$750.0^{+16.4}_{-17.7}$	730.1 ± 15.4	$746.9^{+13.9}_{-14.6}$	755.6 ± 9.6	$754.8^{+20.9}_{-12.3}$
σ_{η}^{-} (pb)						
0.00–0.20	$569.0 \pm 0.6 \pm 5.3 \pm 14.8$	$574.5^{+14.5}_{-20.2}$	562.2 ± 13.3	$576.2^{+9.4}_{-10.1}$	580.2 ± 7.2	$578.8^{+4.1}_{-7.6}$
0.20–0.40	$568.9 \pm 0.6 \pm 6.4 \pm 14.8$	$571.0^{+14.6}_{-20.1}$	559.6 ± 13.3	$573.2^{+9.6}_{-10.3}$	577.4 ± 7.4	$576.1^{+5.0}_{-8.1}$
0.40–0.60	$564.1 \pm 0.6 \pm 5.7 \pm 14.7$	$566.4^{+14.2}_{-19.3}$	555.6 ± 12.8	$569.7^{+8.8}_{-9.3}$	572.6 ± 6.9	$572.5^{+4.1}_{-7.2}$
0.60–0.80	$556.1 \pm 0.6 \pm 5.5 \pm 14.5$	$558.6^{+13.7}_{-18.3}$	547.5 ± 12.4	$561.8^{+8.6}_{-8.9}$	565.9 ± 7.2	$565.7^{+5.8}_{-8.0}$
0.80–1.00	$549.6 \pm 0.6 \pm 5.5 \pm 14.3$	$548.6^{+13.4}_{-17.3}$	538.8 ± 11.7	$553.6^{+8.3}_{-8.3}$	557.9 ± 7.0	$557.4^{+4.9}_{-7.0}$
1.00–1.20	$535.7 \pm 0.6 \pm 4.6 \pm 13.9$	$535.6^{+12.8}_{-16.0}$	526.6 ± 11.6	$542.2^{+8.0}_{-8.1}$	544.2 ± 6.8	$547.2^{+5.3}_{-7.0}$
1.20–1.40	$521.4 \pm 0.6 \pm 4.6 \pm 13.6$	$521.8^{+12.4}_{-14.9}$	512.4 ± 10.9	$527.5^{+8.0}_{-8.2}$	530.9 ± 6.6	$534.5^{+5.3}_{-7.0}$
1.40–1.60	$508.3 \pm 0.6 \pm 4.9 \pm 13.2$	$509.3^{+11.8}_{-13.9}$	500.6 ± 10.5	$516.3^{+8.2}_{-8.4}$	519.3 ± 6.5	$524.2^{+5.4}_{-6.7}$
1.60–1.85	$487.7 \pm 0.6 \pm 5.2 \pm 12.7$	$485.1^{+11.2}_{-12.6}$	478.1 ± 9.9	$492.5^{+8.6}_{-8.8}$	494.6 ± 6.0	$501.6^{+6.3}_{-6.6}$
1.85–2.10	$466.6 \pm 0.6 \pm 5.3 \pm 12.1$	$467.0^{+11.0}_{-11.7}$	459.9 ± 9.4	$473.8^{+9.1}_{-9.4}$	475.1 ± 5.6	$483.4^{+8.7}_{-7.3}$
2.10–2.40	$439.8 \pm 0.6 \pm 10.6 \pm 11.4$	$436.0^{+10.6}_{-11.1}$	431.0 ± 9.0	$442.3^{+9.1}_{-9.4}$	442.0 ± 5.3	$452.4^{+10.1}_{-6.6}$
\mathcal{A} (%)						
0.00–0.20	$13.31 \pm 0.06 \pm 0.17$	$13.89^{+0.55}_{-0.57}$	13.68 ± 0.25	$13.16^{+0.48}_{-0.30}$	13.69 ± 0.20	$13.71^{+0.50}_{-0.43}$
0.20–0.40	$13.70 \pm 0.06 \pm 0.18$	$14.28^{+0.56}_{-0.59}$	13.94 ± 0.23	$13.48^{+0.49}_{-0.30}$	14.04 ± 0.20	$14.07^{+0.51}_{-0.44}$
0.40–0.60	$14.27 \pm 0.06 \pm 0.18$	$14.83^{+0.56}_{-0.60}$	14.47 ± 0.21	$13.92^{+0.48}_{-0.30}$	14.66 ± 0.23	$14.58^{+0.53}_{-0.45}$
0.60–0.80	$15.18 \pm 0.06 \pm 0.18$	$15.85^{+0.55}_{-0.61}$	15.40 ± 0.19	$14.93^{+0.49}_{-0.30}$	15.52 ± 0.21	$15.42^{+0.54}_{-0.47}$
0.80–1.00	$16.19 \pm 0.06 \pm 0.19$	$17.01^{+0.57}_{-0.64}$	16.44 ± 0.19	$15.95^{+0.50}_{-0.31}$	16.59 ± 0.22	$16.49^{+0.58}_{-0.50}$
1.00–1.20	$17.69 \pm 0.07 \pm 0.20$	$18.44^{+0.55}_{-0.65}$	17.92 ± 0.19	$17.31^{+0.51}_{-0.34}$	18.11 ± 0.21	$17.69^{+0.58}_{-0.51}$
1.20–1.40	$19.52 \pm 0.07 \pm 0.22$	$20.14^{+0.56}_{-0.67}$	19.52 ± 0.20	$19.03^{+0.53}_{-0.38}$	19.70 ± 0.23	$19.13^{+0.62}_{-0.54}$
1.40–1.60	$20.75 \pm 0.07 \pm 0.23$	$21.82^{+0.56}_{-0.68}$	21.10 ± 0.21	$20.59^{+0.55}_{-0.42}$	21.26 ± 0.23	$20.63^{+0.60}_{-0.54}$
1.60–1.85	$22.83 \pm 0.06 \pm 0.23$	$23.57^{+0.55}_{-0.68}$	22.84 ± 0.23	$22.50^{+0.57}_{-0.48}$	23.14 ± 0.23	$22.26^{+0.63}_{-0.55}$
1.85–2.10	$24.61 \pm 0.06 \pm 0.22$	$25.43^{+0.54}_{-0.67}$	24.74 ± 0.25	$24.44^{+0.57}_{-0.52}$	24.99 ± 0.24	$24.01^{+0.69}_{-0.60}$
2.10–2.40	$25.96 \pm 0.07 \pm 0.21$	$26.47^{+0.50}_{-0.62}$	25.75 ± 0.28	$25.61^{+0.57}_{-0.55}$	26.19 ± 0.29	$25.05^{+0.78}_{-0.67}$

cantly improved, as illustrated in Fig. 4 where the x_u and x_d valence distributions are shown at the scale of m_W^2 , relevant for the W boson production. The changes in shapes

and the reduction of the uncertainties of the valence quark distributions with respect to those obtained with the HERA data are clear.

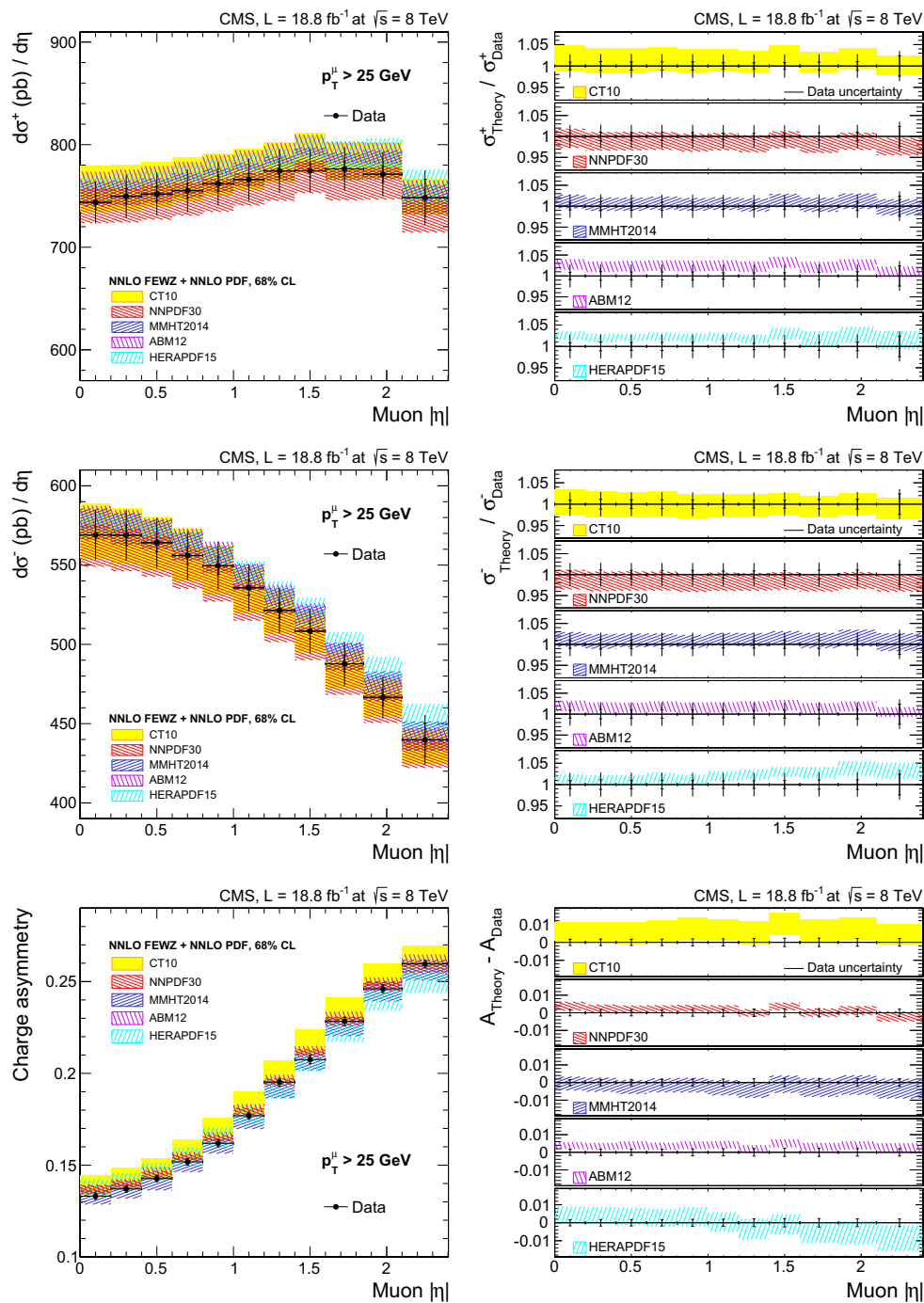


Fig. 3 Comparison of the measured cross sections (*upper plot* for σ_{η}^{+} and middle for σ_{η}^{-}) and asymmetries (*lower plot*) to NNLO predictions calculated using the FEWZ 3.1 MC tool interfaced with different PDF sets. The *right column* shows the ratios (differences) between the theoretical predictions and the measured cross sections (asymmetries).

For direct comparison to the results of the earlier CMS QCD analysis [11] based on the W asymmetry measured at $\sqrt{s} = 7$ TeV and the subset of HERA DIS data [56], an alternative PDF fit is performed at NLO, following exactly the

The *smaller vertical error bars* on the data points represent the statistical and systematic uncertainties. The *full error bars* include the integrated luminosity uncertainty. The PDF uncertainty of each PDF set is shown by a *shaded* (or *hatched*) band and corresponds to 68 % CL

data and model inputs of Ref. [11], but replacing the CMS measurements at $\sqrt{s} = 7$ TeV by those at $\sqrt{s} = 8$ TeV. Also, a combined QCD analysis of both CMS data sets is performed. Very good agreement is observed between the

Table 5 Partial χ^2 per number of data points, n_{dp} , and the global χ^2 per degrees of freedom, n_{dof} , as obtained in the QCD analysis of HERA DIS and the CMS muon charge asymmetry data. For HERA measurements, the energy of the proton beam is listed for each data set, with electron energy being $E_e = 27.5$ GeV

Data sets	Partial χ^2/n_{dp}
HERA1+2 neutral current, e^+p , $E_p = 920$ GeV	440/377
HERA1+2 neutral current, e^+p , $E_p = 820$ GeV	69/70
HERA1+2 neutral current, e^+p , $E_p = 575$ GeV	214/254
HERA1+2 neutral current, e^+p , $E_p = 460$ GeV	210/204
HERA1+2 neutral current, e^-p , $E_p = 920$ GeV	218/159
HERA1+2 charged current, e^+p , $E_p = 920$ GeV	46/39
HERA1+2 charged current, e^-p , $E_p = 920$ GeV	50/42
Correlated χ^2 of HERA1+2 data	141
CMS W^\pm muon charge asymmetry $\mathcal{A}(\eta_\mu)$, $\sqrt{s} = 8$ TeV	3/11
Global χ^2/n_{dof}	1391/1143

CMS measurements of W asymmetry at $\sqrt{s} = 7$ TeV and $\sqrt{s} = 8$ TeV and a similar effect on the central values of the PDFs as reported in Ref. [11]. Compared to the PDFs obtained with HERA only data, the improvement of the precision in the valence quark distributions is more pronounced, when the measurements at $\sqrt{s} = 8$ TeV are used compared

to the results of Ref. [11]. Due to somewhat lower Bjorken x probed by the measurements at 8 TeV, as compared to 7 TeV, the two data sets are complementary and should both be used in the future global QCD analyses.

9 Summary

In summary, we have measured the differential cross section and charge asymmetry of the $W^\pm \rightarrow \mu^\pm \nu$ production in pp collisions at $\sqrt{s} = 8$ TeV using a data sample corresponding to an integrated luminosity of 18.8 fb^{-1} collected with the CMS detector at the LHC. The measurements were performed in 11 bins of absolute muon pseudorapidity $|\eta|$ for muons with $p_T > 25$ GeV. The results have been incorporated into a QCD analysis at next-to-next-to-leading-order together with the inclusive deep inelastic scattering data from HERA. A significant improvement in the accuracy of the valence quark distributions is observed in the range $10^{-3} < x < 10^{-1}$, demonstrating the power of these muon charge asymmetry measurements to improve the main constraints on the valence distributions imposed by the HERA data, in the kinematics range probed. This strongly suggests the use of these measurements in future PDF determinations.

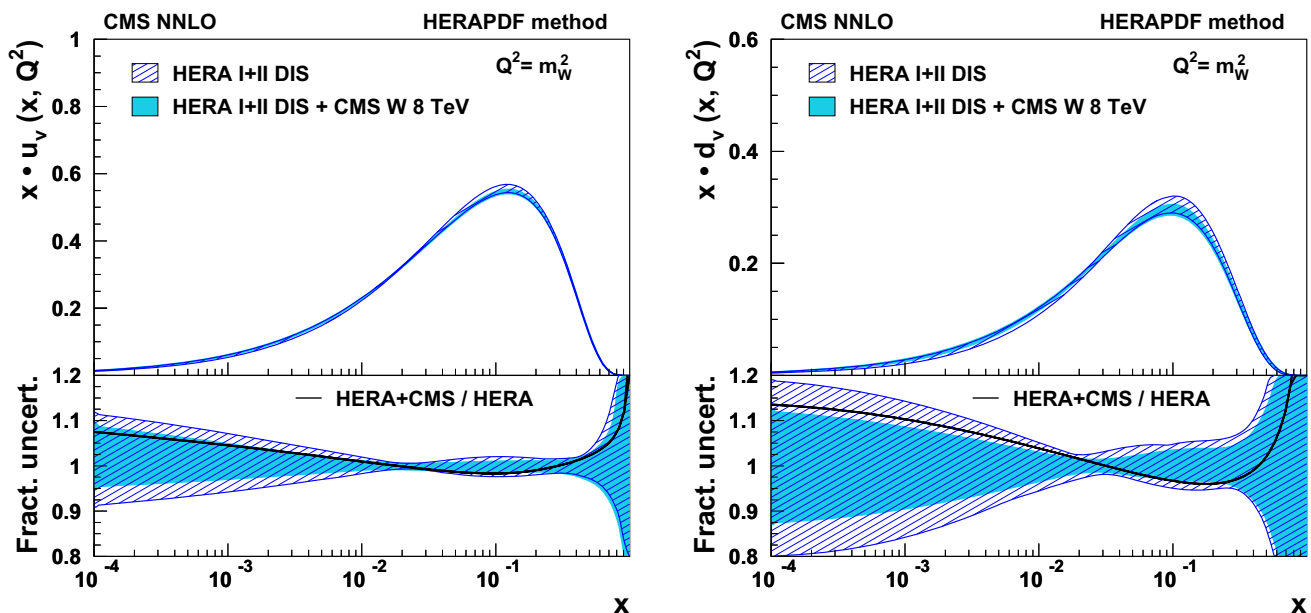


Fig. 4 Distributions of u valence (left) and d valence (right) quarks as functions of x at the scale $Q^2 = m_W^2$. The results of the fit to the HERA data and muon asymmetry measurements (light shaded band), and to HERA data only (hatched band) are compared. The total PDF

uncertainties are shown. In the bottom panels the distributions are normalized to 1 for a direct comparison of the uncertainties. The change of the PDFs with respect to the HERA-only fit is represented by a solid line

Acknowledgments We congratulate our colleagues in the CERN accelerator departments for the excellent performance of the LHC and thank the technical and administrative staffs at CERN and at other CMS institutes for their contributions to the success of the CMS effort. In addition, we gratefully acknowledge the computing centres and personnel of the Worldwide LHC Computing Grid for delivering so effectively the computing infrastructure essential to our analyses. Finally, we acknowledge the enduring support for the construction and operation of the LHC and the CMS detector provided by the following funding agencies: BMWFW and FWF (Austria); FNRS and FWO (Belgium); CNPq, CAPES, FAPERJ, and FAPESP (Brazil); MES (Bulgaria); CERN; CAS, MoST, and NSFC (China); COLCIENCIAS (Colombia); MSES and CSF (Croatia); RPF (Cyprus); MoER, ERC IUT and ERDF (Estonia); Academy of Finland, MEC, and HIP (Finland); CEA and CNRS/IN2P3 (France); BMBF, DFG, and HGF (Germany); GSRT (Greece); OTKA and NIH (Hungary); DAE and DST (India); IPM (Iran); SFI (Ireland); INFN (Italy); MSIP and NRF (Republic of Korea); LAS (Lithuania); MOE and UM (Malaysia); CINVESTAV, CONACYT, SEP, and UASLP-FAI (Mexico); MBIE (New Zealand); PAEC (Pakistan); MSHE and NSC (Poland); FCT (Portugal); JINR (Dubna); MON, RosAtom, RAS and RFBR (Russia); MESTD (Serbia); SEIDI and CPAN (Spain); Swiss Funding Agencies (Switzerland); MST (Taipei); ThEPCenter, IPST, STAR and NSTDA (Thailand); TUBITAK and TAEK (Turkey); NASU and SFFR (Ukraine); STFC (United Kingdom); DOE and NSF (USA). Individuals have received support from the Marie-Curie programme and the European Research Council and EPLANET (European Union); the Leventis Foundation; the A. P. Sloan Foundation; the Alexander von Humboldt Foundation; the Belgian Federal Science Policy Office; the Fonds pour la Formation à la Recherche dans l'Industrie et dans l'Agriculture (FRIA-Belgium); the Agentschap voor Innovatie door Wetenschap en Technologie (IWT-Belgium); the Ministry of Education, Youth and Sports (MEYS) of the Czech Republic; the Council of Science and Industrial Research, India; the HOMING PLUS programme of the Foundation for Polish Science, cofinanced from European Union, Regional Development Fund; the OPUS programme of the National Science Center (Poland); the Compagnia di San Paolo (Torino); MIUR project 20108T4XTM (Italy); the Thalís and Aristeia programmes cofinanced by EU-ESF and the Greek NSRF; the National Priorities Research Program by Qatar National Research Fund; the Rachadapisek Sompot Fund for Postdoctoral Fellowship, Chulalongkorn University (Thailand); the Chulalongkorn Academic into Its Second Century Project Advancement Project (Thailand); and the Welch Foundation, contract C-1845.

Open Access This article is distributed under the terms of the Creative Commons Attribution 4.0 International License (<http://creativecommons.org/licenses/by/4.0/>), which permits unrestricted use, distribution, and reproduction in any medium, provided you give appropriate credit to the original author(s) and the source, provide a link to the Creative Commons license, and indicate if changes were made. Funded by SCOAP³.

References

1. J.D. Bjorken, E.A. Paschos, Inelastic electron-proton and γ -proton scattering and the structure of the nucleon. *Phys. Rev.* **185**, 1975 (1969). doi:[10.1103/PhysRev.185.1975](https://doi.org/10.1103/PhysRev.185.1975)
2. CDF Collaboration, Measurement of the lepton charge asymmetry in W boson decays produced in $p\bar{p}$ collisions. *Phys. Rev. Lett.* **81**, 5754 (1998). doi:[10.1103/PhysRevLett.81.5754](https://doi.org/10.1103/PhysRevLett.81.5754). arXiv:[hep-ex/9809001](https://arxiv.org/abs/hep-ex/9809001)
3. CDF Collaboration, Direct measurement of the W production charge asymmetry in $p\bar{p}$ Collisions at $\sqrt{s} = 1.96\text{TeV}$. *Phys. Rev. Lett.* **102**, 181801 (2009). doi:[10.1103/PhysRevLett.102.181801](https://doi.org/10.1103/PhysRevLett.102.181801). arXiv:[0901.2169](https://arxiv.org/abs/0901.2169)
4. D0 Collaboration, Measurement of the muon charge asymmetry from W boson decays. *Phys. Rev. D* **77**, 011106 (2008). doi:[10.1103/PhysRevD.77.011106](https://doi.org/10.1103/PhysRevD.77.011106). arXiv:[0709.4254](https://arxiv.org/abs/0709.4254)
5. D0 Collaboration, Measurement of the electron charge asymmetry in $p\bar{p} \rightarrow W + X \rightarrow e\nu + X$ events at $\sqrt{s} = 1.96\text{TeV}$. *Phys. Rev. Lett.* **101**, 211801 (2008). doi:[10.1103/PhysRevLett.101.211801](https://doi.org/10.1103/PhysRevLett.101.211801). arXiv:[0807.3367](https://arxiv.org/abs/0807.3367)
6. D0 Collaboration, Measurement of the muon charge asymmetry in $p\bar{p} \rightarrow W + X \rightarrow \mu\nu + X$ events at $\sqrt{s} = 1.96\text{TeV}$. *Phys. Rev. D* **88**, 091102 (2013). doi:[10.1103/PhysRevD.88.091102](https://doi.org/10.1103/PhysRevD.88.091102). arXiv:[1309.2591](https://arxiv.org/abs/1309.2591)
7. CMS Collaboration, Measurement of the lepton charge asymmetry in inclusive W production in pp collisions at $\sqrt{s} = 7\text{TeV}$. *JHEP* **04**, 050 (2011). doi:[10.1007/JHEP04\(2011\)050](https://doi.org/10.1007/JHEP04(2011)050). arXiv:[1103.3470](https://arxiv.org/abs/1103.3470)
8. ATLAS Collaboration, Measurement of the inclusive W^\pm and Z/γ cross sections in the e and μ decay channels in pp collisions at $\sqrt{s} = 7\text{TeV}$ with the ATLAS detector. *Phys. Rev. D* **85**, 072004 (2012). doi:[10.1103/PhysRevD.85.072004](https://doi.org/10.1103/PhysRevD.85.072004). arXiv:[1109.5141](https://arxiv.org/abs/1109.5141)
9. LHCb Collaboration, Inclusive W and Z production in the forward region at $\sqrt{s} = 7\text{TeV}$. *JHEP* **06**, 058 (2012). doi:[10.1007/JHEP06\(2012\)058](https://doi.org/10.1007/JHEP06(2012)058). arXiv:[1204.1620](https://arxiv.org/abs/1204.1620)
10. CMS Collaboration, Measurement of the Electron charge asymmetry in inclusive W production in pp collisions at $\sqrt{s} = 7\text{TeV}$. *Phys. Rev. Lett.* **109**, 111806 (2012). doi:[10.1103/PhysRevLett.109.111806](https://doi.org/10.1103/PhysRevLett.109.111806). arXiv:[1206.2598](https://arxiv.org/abs/1206.2598)
11. CMS Collaboration, Measurement of the muon charge asymmetry in inclusive $pp \rightarrow W + X$ production at $\sqrt{s} = 7\text{TeV}$ and an improved determination of light parton distribution functions. *Phys. Rev. D* **90**, 032004 (2014). doi:[10.1103/PhysRevD.90.032004](https://doi.org/10.1103/PhysRevD.90.032004). arXiv:[1312.6283](https://arxiv.org/abs/1312.6283)
12. CMS Collaboration, The CMS experiment at the CERN LHC. *JINST* **3**, S08004 (2008). doi:[10.1088/1748-0221/3/08/S08004](https://doi.org/10.1088/1748-0221/3/08/S08004)
13. S. Alioli, P. Nason, C. Oleari, E. Re, NLO vector-boson production matched with shower in POWHEG. *JHEP* **07**, 060 (2008). doi:[10.1088/1126-6708/2008/07/060](https://doi.org/10.1088/1126-6708/2008/07/060). arXiv:[0805.4802](https://arxiv.org/abs/0805.4802)
14. P. Nason, A new method for combining NLO QCD with shower Monte Carlo algorithms. *JHEP* **11**, 040 (2004). doi:[10.1088/1126-6708/2004/11/040](https://doi.org/10.1088/1126-6708/2004/11/040). arXiv:[hep-ph/0409146](https://arxiv.org/abs/hep-ph/0409146)
15. S. Frixione, P. Nason, C. Oleari, Matching NLO QCD computations with parton shower simulations: the POWHEG method. *JHEP* **11**, 070 (2007). doi:[10.1088/1126-6708/2007/11/070](https://doi.org/10.1088/1126-6708/2007/11/070). arXiv:[0709.2092](https://arxiv.org/abs/0709.2092)
16. S. Alioli, P. Nason, C. Oleari, E. Re, A general framework for implementing NLO calculations in shower Monte Carlo programs: the POWHEG BOX. *JHEP* **06**, 043 (2010). doi:[10.1007/JHEP06\(2010\)043](https://doi.org/10.1007/JHEP06(2010)043). arXiv:[1002.2581](https://arxiv.org/abs/1002.2581)
17. T. Sjöstrand, S. Mrenna, P. Skands, PYTHIA 6.4 physics and manual. *JHEP* **15**, 026 (2006). doi:[10.1088/1126-6708/2006/05/026](https://doi.org/10.1088/1126-6708/2006/05/026). arXiv:[hep-ph/0603175](https://arxiv.org/abs/hep-ph/0603175)
18. H.-L. Lai et al., New parton distributions for collider physics. *Phys. Rev. D* **82**, 074024 (2010). doi:[10.1103/PhysRevD.82.074024](https://doi.org/10.1103/PhysRevD.82.074024). arXiv:[1007.2241](https://arxiv.org/abs/1007.2241)
19. N. Davidson et al., Universal interface of TAUOLA technical and physics documentation. *Comput. Phys. Commun.* **183**, 821 (2012). doi:[10.1016/j.cpc.2011.12.009](https://doi.org/10.1016/j.cpc.2011.12.009). arXiv:[1002.0543](https://arxiv.org/abs/1002.0543)
20. J. Pumplin et al., New generation of parton distributions with uncertainties from global QCD analysis. *JHEP* **07**, 012 (2002). doi:[10.1088/1126-6708/2002/07/012](https://doi.org/10.1088/1126-6708/2002/07/012). arXiv:[hep-ph/0201195](https://arxiv.org/abs/hep-ph/0201195)
21. GEANT4 Collaboration, GEANT4—a simulation toolkit. *Nucl. Instrum. Meth. A* **506**, 250 (2003). doi:[10.1016/S0168-9002\(03\)01368-8](https://doi.org/10.1016/S0168-9002(03)01368-8)
22. A. Bodek et al., Extracting muon momentum scale corrections for hadron collider experiments. *Eur. Phys. J. C* **72**, 2194 (2012). doi:[10.1140/epjc/s10052-012-2194-8](https://doi.org/10.1140/epjc/s10052-012-2194-8). arXiv:[1208.3710](https://arxiv.org/abs/1208.3710)

23. CMS Collaboration, Measurements of inclusive W and Z cross sections in pp collisions at $\sqrt{s} = 7\text{TeV}$ with the CMS experiment. JHEP **10**, 132 (2011). doi:[10.1007/JHEP10\(2011\)132](https://doi.org/10.1007/JHEP10(2011)132). arXiv:[1107.4789](https://arxiv.org/abs/1107.4789)
24. CMS Collaboration, Performance of CMS muon reconstruction in pp collision events at $\sqrt{s} = 7\text{TeV}$. JINST **7**, P10002 (2012). doi:[10.1088/1748-0221/7/10/P10002](https://doi.org/10.1088/1748-0221/7/10/P10002). arXiv:[1206.4071](https://arxiv.org/abs/1206.4071)
25. CMS Collaboration, Particle-flow event reconstruction in CMS and performance for jets, taus, and E_T^{miss} . CMS Physics Analysis Summary CMS-PAS-PFT-09-001, CERN, 2009
26. CMS Collaboration, Commissioning of the particle-flow event reconstruction with the first LHC collisions recorded in the CMS detector. CMS Physics Analysis Summary CMS-PAS-PFT-10-001, CERN, 2010
27. CMS Collaboration, Performance of the CMS missing transverse momentum reconstruction in pp data at $\sqrt{s} = 8\text{TeV}$. JINST **10**, P02006 (2015). doi:[10.1088/1748-0221/10/02/P02006](https://doi.org/10.1088/1748-0221/10/02/P02006). arXiv:[1411.0511](https://arxiv.org/abs/1411.0511)
28. D0 Collaboration, A novel method for modeling the recoil in W boson events at hadron collider. Nucl. Instrum. Meth. A **609**, 250 (2009). doi:[10.1016/j.nima.2009.08.056](https://doi.org/10.1016/j.nima.2009.08.056). arXiv:[0907.3713](https://arxiv.org/abs/0907.3713)
29. CMS Collaboration, Missing transverse energy performance of the CMS detector. JINST **6**, P09001 (2011). doi:[10.1088/1748-0221/6/09/P09001](https://doi.org/10.1088/1748-0221/6/09/P09001). arXiv:[1106.5048](https://arxiv.org/abs/1106.5048)
30. M. Czakon, A. Mitov, Top++: a program for the calculation of the top-pair cross-section at hadron colliders. Comput. Phys. Commun. **185**, 2930 (2014). doi:[10.1016/j.cpc.2014.06.021](https://doi.org/10.1016/j.cpc.2014.06.021). arXiv:[1112.5675](https://arxiv.org/abs/1112.5675)
31. Particle Data Group Collaboration, Review of particle physics. Chin. Phys. C **38**, 090001 (2014). doi:[10.1088/1674-1137/38/9/090001](https://doi.org/10.1088/1674-1137/38/9/090001)
32. G. Nanava, Z. Was, How to use SANC to improve the PHOTOS Monte Carlo simulation of bremsstrahlung in leptonic W boson decays. Acta Phys. Polon. B **34**, 4561 (2003). arXiv:[hep-ph/0303260](https://arxiv.org/abs/hep-ph/0303260)
33. H. Burkhardt, B. Pietrzyk, Update of the hadronic contribution to the QED vacuum polarization. Phys. Lett. B **513**, 46 (2001). doi:[10.1016/S0370-2693\(01\)00393-8](https://doi.org/10.1016/S0370-2693(01)00393-8)
34. A.D. Martin, W.J. Stirling, R.S. Thorne, G. Watt, Parton distributions for the LHC. Eur. Phys. J. C **63**, 189 (2009). doi:[10.1140/epjc/s10052-009-1072-5](https://doi.org/10.1140/epjc/s10052-009-1072-5). arXiv:[0901.0002](https://arxiv.org/abs/0901.0002)
35. NNPDF Collaboration, Impact of heavy quark masses on parton distributions and LHC phenomenology. Nucl. Phys. B **849**, 296 (2011). doi:[10.1016/j.nuclphysb.2011.03.021](https://doi.org/10.1016/j.nuclphysb.2011.03.021). arXiv:[1101.1300](https://arxiv.org/abs/1101.1300)
36. CMS Collaboration, CMS luminosity based on pixel cluster counting—summer 2013 update. CMS Physics Analysis Summary CMS-PAS-LUM-13-001, CERN, 2013
37. Y. Li, F. Petriello, Combining QCD and electroweak corrections to dilepton production in the framework of the FEWZ simulation code. Phys. Rev. D **86**, 094034 (2012). doi:[10.1103/PhysRevD.86.094034](https://doi.org/10.1103/PhysRevD.86.094034). arXiv:[1208.5967](https://arxiv.org/abs/1208.5967)
38. NNPDF Collaboration, Parton distributions for the LHC Run II. JHEP **04**, 040 (2015). doi:[10.1007/JHEP04\(2015\)040](https://doi.org/10.1007/JHEP04(2015)040). arXiv:[1410.8849](https://arxiv.org/abs/1410.8849)
39. H1 and ZEUS Collaborations, in *Combination and QCD Analysis of the HERA Inclusive Cross Sections*. Proceedings of the 35th International Conference of High Energy Physics, vol. 168. 2010. PoS(ICHEP2010)168. Grids available at http://www.desy.de/h1zeus/combined_results/index.php?do=proton_structure. Accessed July 2010
40. L.A. Harland-Lang, A.D. Martin, P. Motylinski, R.S. Thorne, Parton distributions in the LHC era: MMHT 2014 PDFs. Eur. Phys. J. C **75**, 204 (2015). doi:[10.1140/epjc/s10052-015-3397-6](https://doi.org/10.1140/epjc/s10052-015-3397-6). arXiv:[1412.3989](https://arxiv.org/abs/1412.3989)
41. S. Alekhin, J. Blumlein, S. Moch, The ABM parton distributions tuned to LHC data. Phys. Rev. D **89**, 054028 (2014). doi:[10.1103/PhysRevD.89.054028](https://doi.org/10.1103/PhysRevD.89.054028). arXiv:[1310.3059](https://arxiv.org/abs/1310.3059)
42. H1 and ZEUS Collaborations, Combination of measurements of inclusive deep inelastic e^+p scattering cross sections and QCD analysis of HERA data. Eur. Phys. J. C **75**, 580 (2015). doi:[10.1140/epjc/s10052-015-3710-4](https://doi.org/10.1140/epjc/s10052-015-3710-4). arXiv:[1506.06042](https://arxiv.org/abs/1506.06042)
43. J.M. Campbell, R.K. Ellis, Update on vector boson pair production at hadron colliders. Phys. Rev. D **60**, 113006 (1999). doi:[10.1103/PhysRevD.60.113006](https://doi.org/10.1103/PhysRevD.60.113006). arXiv:[hep-ph/9905386](https://arxiv.org/abs/hep-ph/9905386)
44. J.M. Campbell, R.K. Ellis, MCFM for the Tevatron and the LHC. Nucl. Phys. Proc. Suppl. **205–206**, 10 (2010). doi:[10.1016/j.nuclphysbps.2010.08.011](https://doi.org/10.1016/j.nuclphysbps.2010.08.011). arXiv:[1007.3492](https://arxiv.org/abs/1007.3492)
45. T. Carli et al., A posteriori inclusion of parton density functions in NLO QCD final-state calculations at hadron colliders: the APPLGRID project. Eur. Phys. J. C **66**, 503 (2010). doi:[10.1140/epjc/s10052-010-1255-0](https://doi.org/10.1140/epjc/s10052-010-1255-0). arXiv:[0911.2985](https://arxiv.org/abs/0911.2985)
46. S. Alekhin et al., HERAFitter. Eur. Phys. J. C **75**, 304 (2015). doi:[10.1140/epjc/s10052-015-3480-z](https://doi.org/10.1140/epjc/s10052-015-3480-z). arXiv:[1410.4412](https://arxiv.org/abs/1410.4412)
47. HERAFitter web site, <http://www.herafitter.org>. Accessed Aug 2015
48. V.N. Gribov, L.N. Lipatov, Deep inelastic $e - p$ scattering in perturbation theory. Sov. J. Nucl. Phys. **15**, 438 (1972)
49. G. Altarelli, G. Parisi, Asymptotic freedom in parton language. Nucl. Phys. B **126**, 298 (1977). doi:[10.1016/0550-3213\(77\)90384-4](https://doi.org/10.1016/0550-3213(77)90384-4)
50. G. Curci, W. Furmanski, R. Petronzio, Evolution of parton densities beyond leading order: the non-singlet case. Nucl. Phys. B **175**, 27 (1980). doi:[10.1016/0550-3213\(80\)90003-6](https://doi.org/10.1016/0550-3213(80)90003-6)
51. W. Furmanski, R. Petronzio, Singlet parton densities beyond leading order. Phys. Lett. B **97**, 437 (1980). doi:[10.1016/0370-2693\(80\)90636-X](https://doi.org/10.1016/0370-2693(80)90636-X)
52. S. Moch, J.A.M. Vermaseren, A. Vogt, The three-loop splitting functions in QCD: the non-singlet case. Nucl. Phys. B **688**, 101 (2004). doi:[10.1016/j.nuclphysb.2004.03.030](https://doi.org/10.1016/j.nuclphysb.2004.03.030). arXiv:[hep-ph/0403192](https://arxiv.org/abs/hep-ph/0403192)
53. A. Vogt, S. Moch, J.A.M. Vermaseren, The three-loop splitting functions in QCD: the singlet case. Nucl. Phys. B **691**, 129 (2004). doi:[10.1016/j.nuclphysb.2004.04.024](https://doi.org/10.1016/j.nuclphysb.2004.04.024). arXiv:[hep-ph/0404111](https://arxiv.org/abs/hep-ph/0404111)
54. M. Botje, QCDNUM: fast QCD evolution and convolution. Comput. Phys. Commun. **182**, 490 (2011). doi:[10.1016/j.cpc.2010.10.020](https://doi.org/10.1016/j.cpc.2010.10.020). arXiv:[1005.1481](https://arxiv.org/abs/1005.1481)
55. R.S. Thorne, Variable-flavor number scheme for NNLO. Phys. Rev. D **73**, 054019 (2006). doi:[10.1103/PhysRevD.73.054019](https://doi.org/10.1103/PhysRevD.73.054019). arXiv:[hep-ph/0601245](https://arxiv.org/abs/hep-ph/0601245)
56. H1 and ZEUS Collaborations, Combined measurement and QCD analysis of the inclusive e^+p scattering cross sections at HERA. JHEP **01**, 109 (2010). doi:[10.1007/JHEP01\(2010\)109](https://doi.org/10.1007/JHEP01(2010)109). arXiv:[0911.0884](https://arxiv.org/abs/0911.0884)

CMS Collaboration**Yerevan Physics Institute, Yerevan, Armenia**

V. Khachatryan, A. M. Sirunyan, A. Tumasyan

Institut für Hochenergiephysik der OeAW, Vienna, Austria

W. Adam, E. Asilar, T. Bergauer, J. Brandstetter, E. Brondolin, M. Dragicevic, J. Erö, M. Flechl, M. Friedl, R. Frühwirth¹,
 V. M. Ghete, C. Hartl, N. Hörmann, J. Hrubec, M. Jeitler¹, A. König, M. Krammer¹, I. Krätschmer, D. Liko, T. Matsushita,
 I. Mikulec, D. Rabadý, N. Rad, B. Rahbaran, H. Rohringer, J. Schieck¹, R. Schöfbeck, J. Strauss, W. Treberer-Treberspurg,
 W. Waltenberger, C.-E. Wulz¹

National Centre for Particle and High Energy Physics, Minsk, Belarus

V. Mossolov, N. Shumeiko, J. Suarez Gonzalez

Universiteit Antwerpen, Antwerpe, Belgium

S. Alderweireldt, T. Cornelis, E. A. De Wolf, X. Janssen, A. Knutsson, J. Lauwers, S. Luyckx, M. Van De Klundert, H. Van Haevermaet, P. Van Mechelen, N. Van Remortel, A. Van Spilbeeck

Vrije Universiteit Brussel, Brussel, Belgium

S. Abu Zeid, F. Blekman, J. D'Hondt, N. Daci, I. De Bruyn, K. Deroover, N. Heracleous, J. Keaveney, S. Lowette,
 S. Moortgat, L. Moreels, A. Olbrechts, Q. Python, D. Strom, S. Tavernier, W. Van Doninck, P. Van Mulders, I. Van Parijs

Université Libre de Bruxelles, Brussel, Belgium

H. Brun, C. Caillol, B. Clerbaux, G. De Lentdecker, G. Fasanella, L. Favart, R. Goldouzian, A. Grebenyuk, G. Karapostoli,
 T. Lenzi, A. Léonard, T. Maerschalk, A. Marinov, A. Randle-conde, T. Seva, C. Vander Velde, P. Vanlaer, R. Yonamine,
 F. Zenoni, F. Zhang²

Ghent University, Ghent, Belgium

L. Benucci, A. Cimmino, S. Crucy, D. Dobur, A. Fagot, G. Garcia, M. Gul, J. McCartin, A. A. Ocampo Rios, D. Poyraz,
 D. Ryckbosch, S. Salva, M. Sigamani, M. Tytgat, W. Van Driessche, E. Yazgan, N. Zaganidis

Université Catholique de Louvain, Louvain-la-Neuve, Belgium

S. Basegmez, C. Beluffi³, O. Bondu, S. Brochet, G. Bruno, A. Caudron, L. Ceard, S. De Visscher, C. Delaere, M. Delcourt,
 D. Favart, L. Forthomme, A. Giammanco, A. Jafari, P. Jez, M. Komm, V. Lemaitre, A. Mertens, M. Musich, C. Nuttens,
 K. Piotrkowski, L. Quertenmont, M. Selvaggi, M. Vidal Marono

Université de Mons, Mons, Belgium

N. Beliy, G. H. Hammad

Centro Brasileiro de Pesquisas Fisicas, Rio de Janeiro, Brazil

W. L. Aldá Júnior, F. L. Alves, G. A. Alves, L. Brito, M. Correa Martins Junior, M. Hamer, C. Hensel, A. Moraes, M. E. Pol,
 P. Rebello Teles

Universidade do Estado do Rio de Janeiro, Rio de Janeiro, Brazil

E. Belchior Batista Das Chagas, W. Carvalho, J. Chinellato⁴, A. Custódio, E. M. Da Costa, D. De Jesus Damiao, C. De
 Oliveira Martins, S. Fonseca De Souza, L. M. Huertas Guativa, H. Malbouisson, D. Matos Figueiredo, C. Mora Herrera,
 L. Mundim, H. Nogima, W. L. Prado Da Silva, A. Santoro, A. Sznajder, E. J. Tonelli Manganote⁴, A. Vilela Pereira

Universidade Estadual Paulista^a, Universidade Federal do ABC^b, São Paulo, Brazil

S. Ahuja^a, C. A. Bernardes^b, A. De Souza Santos^b, S. Dogra^a, T. R. Fernandez Perez Tomei^a, E. M. Gregores^b,
 P. G. Mercadante^b, C. S. Moon^{a,5}, S. F. Novaes^a, Sandra S. Padula^a, D. Romero Abad^b, J. C. Ruiz Vargas

Institute for Nuclear Research and Nuclear Energy, Sofia, Bulgaria

A. Aleksandrov, R. Hadjiiska, P. Iaydjiev, M. Rodozov, S. Stoykova, G. Sultanov, M. Vutova

University of Sofia, Sofia, Bulgaria

A. Dimitrov, I. Glushkov, L. Litov, B. Pavlov, P. Petkov

Beihang University, Beijing, ChinaW. Fang⁶

Institute of High Energy Physics, Beijing, China

M. Ahmad, J. G. Bian, G. M. Chen, H. S. Chen, M. Chen, T. Cheng, R. Du, C. H. Jiang, D. Leggat, R. Plestina⁷, F. Romeo, S. M. Shaheen, A. Spiezia, J. Tao, C. Wang, Z. Wang, H. Zhang

State Key Laboratory of Nuclear Physics and Technology, Peking University, Beijing, China

C. Asawatangtrakuldee, Y. Ban, Q. Li, S. Liu, Y. Mao, S. J. Qian, D. Wang, Z. Xu

Universidad de Los Andes, Bogotá, Colombia

C. Avila, A. Cabrera, L. F. Chaparro Sierra, C. Florez, J. P. Gomez, B. Gomez Moreno, J. C. Sanabria

Faculty of Electrical Engineering, Mechanical Engineering and Naval Architecture, University of Split, Split, Croatia

N. Godinovic, D. Lelas, I. Puljak, P. M. Ribeiro Cipriano

Faculty of Science, University of Split, Split, Croatia

Z. Antunovic, M. Kovac

Institute Rudjer Boskovic, Zagreb, Croatia

V. Brigljevic, K. Kadija, J. Luetic, S. Micanovic, L. Sudic

University of Cyprus, Nicosia, Cyprus

A. Attikis, G. Mavromanolakis, J. Mousa, C. Nicolaou, F. Ptochos, P. A. Razis, H. Rykaczewski

Charles University, Prague, Czech Republic

M. Finger⁸, M. Finger Jr.⁸

Universidad San Francisco de Quito, Quito, Ecuador

E. Carrera Jarrin

Academy of Scientific Research and Technology of the Arab Republic of Egypt, Egyptian Network of High Energy Physics, Cairo, Egypt

A. A. Abdelalim^{9,10}, E. El-khateeb¹¹, T. Elkafrawy¹¹, M. A. Mahmoud^{12,13}

National Institute of Chemical Physics and Biophysics, Tallinn, Estonia

B. Calpas, M. Kadastik, M. Murumaa, L. Perrini, M. Raidal, A. Tiko, C. Veelken

Department of Physics, University of Helsinki, Helsinki, Finland

P. Eerola, J. Pekkanen, M. Voutilainen

Helsinki Institute of Physics, Helsinki, Finland

J. Härkönen, V. Karimäki, R. Kinnunen, T. Lampén, K. Lassila-Perini, S. Lehti, T. Lindén, P. Luukka, T. Peltola, J. Tuominiemi, E. Tuovinen, L. Wendland

Lappeenranta University of Technology, Lappeenranta, Finland

J. Talvitie, T. Tuuva

DSM/IRFU, CEA/Saclay, Gif-sur-Yvette, France

M. Besancon, F. Couderc, M. Dejjardin, D. Denegri, B. Fabbro, J. L. Faure, C. Favaro, F. Ferri, S. Ganjour, A. Givernaud, P. Gras, G. Hamel de Monchenault, P. Jarry, E. Locci, M. Machet, J. Malcles, J. Rander, A. Rosowsky, M. Titov, A. Zghiche

Laboratoire Leprince-Ringuet, Ecole Polytechnique, IN2P3-CNRS, Palaiseau, France

A. Abdulsalam, I. Antropov, S. Baffioni, F. Beaudette, P. Busson, L. Cadamuro, E. Chapon, C. Charlot, O. Davignon, R. Granier de Cassagnac, M. Jo, S. Lisniak, P. Miné, I. N. Naranjo, M. Nguyen, C. Ochando, G. Ortona, P. Paganini, P. Pigard, S. Regnard, R. Salerno, Y. Sirois, T. Strebler, Y. Yilmaz, A. Zabi

Institut Pluridisciplinaire Hubert Curien, Université de Strasbourg, Université de Haute Alsace Mulhouse, CNRS/IN2P3, Strasbourg, France

J.-L. Agram¹⁴, J. Andrea, A. Aubin, D. Bloch, J.-M. Brom, M. Buttignol, E. C. Chabert, N. Chanon, C. Collard, E. Conte¹⁴, X. Coubez, J.-C. Fontaine¹⁴, D. Gelé, U. Goerlach, C. Goetzmann, A.-C. Le Bihan, J. A. Merlin¹⁵, K. Skovpen, P. Van Hove

Centre de Calcul de l'Institut National de Physique Nucleaire et de Physique des Particules CNRS/IN2P3, Villeurbanne, France

S. Gadrat

Université de Lyon, Université Claude Bernard Lyon 1, CNRS-IN2P3, Institut de Physique Nucléaire de Lyon, Villeurbanne, France

S. Beauceron, C. Bernet, G. Boudoul, E. Bouvier, C. A. Carrillo Montoya, R. Chierici, D. Contardo, B. Courbon, P. Depasse, H. El Mamouni, J. Fan, J. Fay, S. Gascon, M. Gouzevitch, B. Ille, F. Lagarde, I. B. Laktineh, M. Lethuillier, L. Mirabito, A. L. Pequegnot, S. Perries, A. Popov¹⁶, J. D. Ruiz Alvarez, D. Sabes, V. Sordini, M. Vander Donckt, P. Verdier, S. Viret

Georgian Technical University, Tbilisi, Georgia

T. Toriashvili¹⁷

Tbilisi State University, Tbilisi, Georgia

D. Lomidze

RWTH Aachen University I. Physikalisches Institut, Aachen, Germany

C. Autermann, S. Beranek, L. Feld, A. Heister, M. K. Kiesel, K. Klein, M. Lipinski, A. Ostapchuk, M. Preuten, F. Raupach, S. Schael, J. F. Schulte, T. Verlage, H. Weber, V. Zhukov¹⁶

RWTH Aachen University III. Physikalisches Institut A, Aachen, Germany

M. Ata, M. Brodski, E. Dietz-Laursonn, D. Duchardt, M. Endres, M. Erdmann, S. Erdweg, T. Esch, R. Fischer, A. Güth, T. Hebbeker, C. Heidemann, K. Hoepfner, S. Knutzen, M. Merschmeyer, A. Meyer, P. Millet, S. Mukherjee, M. Olschewski, K. Padeken, P. Papacz, T. Pook, M. Radziej, H. Reithler, M. Rieger, F. Scheuch, L. Sonnenschein, D. Teyssier, S. Thüer

RWTH Aachen University III. Physikalisches Institut B, Aachen, Germany

V. Cherepanov, Y. Erdogan, G. Flügge, H. Geenen, M. Geisler, F. Hoehle, B. Kargoll, T. Kress, A. Künsken, J. Lingemann, A. Nehrkorn, A. Nowack, I. M. Nugent, C. Pistone, O. Pooth, A. Stahl¹⁵

Deutsches Elektronen-Synchrotron, Hamburg, Germany

M. Aldaya Martin, I. Asin, K. Beernaert, O. Behnke, U. Behrens, K. Borras¹⁸, A. Burgmeier, A. Campbell, C. Contreras-Campana, F. Costanza, C. Diez Pardos, G. Dolinska, S. Dooling, G. Eckerlin, D. Eckstein, T. Eichhorn, E. Eren, E. Gallo¹⁹, J. Garay Garcia, A. Geiser, A. Gizhko, P. Gunnellini, J. Hauk, M. Hempel²⁰, H. Jung, A. Kalogeropoulos, O. Karacheban²⁰, M. Kasemann, P. Katsas, J. Kieseler, C. Kleinwort, I. Korol, W. Lange, J. Leonard, K. Lipka, A. Lobanov, W. Lohmann²⁰, R. Mankel, I.-A. Melzer-Pellmann, A. B. Meyer, G. Mittag, J. Mnich, A. Mussgiller, A. Nayak, E. Ntomari, D. Pitzl, R. Placakyte, A. Raspereza, B. Roland, M.Ö. Sahin, P. Saxena, T. Schoerner-Sadenius, C. Seitz, S. Spannagel, N. Stefaniuk, K. D. Trippkewitz, G. P. Van Onsem, R. Walsh, C. Wissing

University of Hamburg, Hamburg, Germany

V. Blobel, M. Centis Vignali, A. R. Draeger, T. Dreyer, J. Erfle, E. Garutti, K. Goebel, D. Gonzalez, M. Görner, J. Haller, M. Hoffmann, R. S. Höing, A. Junkes, R. Klanner, R. Kogler, N. Kovalchuk, T. Lapsien, T. Lenz, I. Marchesini, D. Marconi, M. Meyer, M. Niedziela, D. Nowatschin, J. Ott, F. Pantaleo¹⁵, T. Peiffer, A. Perieanu, N. Pietsch, J. Poehlsen, C. Sander, C. Scharf, P. Schleper, E. Schlieckau, A. Schmidt, S. Schumann, J. Schwandt, H. Stadie, G. Steinbrück, F. M. Stober, H. Tholen, D. Troendle, E. Usai, L. Vanelderen, A. Vanhoefer, B. Vormwald

Institut für Experimentelle Kernphysik, Karlsruhe, Germany

C. Barth, C. Baus, J. Berger, C. Böser, E. Butz, T. Chwalek, F. Colombo, W. De Boer, A. Descroix, A. Dierlamm, S. Fink, F. Frensch, R. Friese, M. Giffels, A. Gilbert, D. Haitz, F. Hartmann¹⁵, S. M. Heindl, U. Husemann, I. Katkov¹⁶, A. Kornmayer¹⁵, P. Lobelle Pardo, B. Maier, H. Mildner, M. U. Mozer, T. Müller, Th. Müller, M. Plagge, G. Quast, K. Rabbertz, S. Röcker, F. Roscher, M. Schröder, G. Sieber, H. J. Simonis, R. Ulrich, J. Wagner-Kuhr, S. Wayand, M. Weber, T. Weiler, S. Williamson, C. Wöhrmann, R. Wolf

Institute of Nuclear and Particle Physics (INPP), NCSR Demokritos, Aghia Paraskevi, Greece

G. Anagnostou, G. Daskalakis, T. Gerasis, V. A. Giakoumopoulou, A. Kyriakis, D. Loukas, A. Psallidas, I. Topsis-Giotis

National and Kapodistrian University of Athens, Athens, Greece

A. Agapitos, S. Kesisoglou, A. Panagiotou, N. Saoulidou, E. Tziaferi

University of Ioánnina, Ioánnina, Greece

I. Evangelou, G. Flouris, C. Foudas, P. Kokkas, N. Loukas, N. Manthos, I. Papadopoulos, E. Paradas, J. Strologas

MTA-ELTE Lendület CMS Particle and Nuclear Physics Group, Eötvös Loránd University, Budapest, Hungary

N. Filipovic

Wigner Research Centre for Physics, Budapest, Hungary

G. Bencze, C. Hajdu, P. Hidas, D. Horvath²¹, F. Sikler, V. Veszpremi, G. Vesztergombi²², A. J. Zsigmond

Institute of Nuclear Research ATOMKI, Debrecen, Hungary

N. Beni, S. Czellar, J. Karancsi²³, J. Molnar, Z. Szillasi

University of Debrecen, Debrecen, Hungary

M. Bartók²², A. Makovec, P. Raics, Z. L. Trocsanyi, B. Ujvari

National Institute of Science Education and Research, Bhubaneswar, India

S. Choudhury²⁴, P. Mal, K. Mandal, D. K. Sahoo, N. Sahoo, S. K. Swain

Panjab University, Chandigarh, India

S. Bansal, S. B. Beri, V. Bhatnagar, R. Chawla, R. Gupta, U. Bhawandeep, A. K. Kalsi, A. Kaur, M. Kaur, R. Kumar, A. Mehta, M. Mittal, J. B. Singh, G. Walia

University of Delhi, Delhi, India

Ashok Kumar, A. Bhardwaj, B. C. Choudhary, R. B. Garg, S. Keshri, A. Kumar, S. Malhotra, M. Naimuddin, N. Nishu, K. Ranjan, R. Sharma, V. Sharma

Saha Institute of Nuclear Physics, Kolkata, India

R. Bhattacharya, S. Bhattacharya, K. Chatterjee, S. Dey, S. Dutta, S. Ghosh, N. Majumdar, A. Modak, K. Mondal, S. Mukhopadhyay, S. Nandan, A. Purohit, A. Roy, D. Roy, S. Roy Chowdhury, S. Sarkar, M. Sharan

Bhabha Atomic Research Centre, Mumbai, India

R. Chudasama, D. Dutta, V. Jha, V. Kumar, A. K. Mohanty¹⁵, L. M. Pant, P. Shukla, A. Topkar

Tata Institute of Fundamental Research, Mumbai, India

T. Aziz, S. Banerjee, S. Bhowmik²⁵, R. M. Chatterjee, R. K. Dewanjee, S. Dugad, S. Ganguly, S. Ghosh, M. Guchait, A. Gurtu²⁶, Sa. Jain, G. Kole, S. Kumar, B. Mahakud, M. Maity²⁵, G. Majumder, K. Mazumdar, S. Mitra, G. B. Mohanty, B. Parida, T. Sarkar²⁵, N. Sur, B. Sutar, N. Wickramage²⁷

Indian Institute of Science Education and Research (IISER), Pune, India

S. Chauhan, S. Dube, A. Kapoor, K. Kotheekar, A. Rane, S. Sharma

Institute for Research in Fundamental Sciences (IPM), Tehran, Iran

H. Bakhshiansohi, H. Behnamian, S. M. Etesami²⁸, A. Fahim²⁹, M. Khakzad, M. Mohammadi Najafabadi, M. Naseri, S. Paktinat Mehdiabadi, F. Rezaei Hosseinabadi, B. Safarzadeh³⁰, M. Zeinali

University College Dublin, Dublin, Ireland

M. Felcini, M. Grunewald

INFN Sezione di Bari^a, Università di Bari^b, Politecnico di Bari^c, Bari, Italy

M. Abbrescia^{a,b}, C. Calabria^{a,b}, C. Caputo^{a,b}, A. Colaleo^a, D. Creanza^{a,c}, L. Cristella^{a,b}, N. De Filippis^{a,c}, M. De Palma^{a,b}, L. Fiore^a, G. Iaselli^{a,c}, G. Maggi^{a,c}, M. Maggi^a, G. Miniello^{a,b}, S. My^{a,b}, S. Nuzzo^{a,b}, A. Pompili^{a,b}, G. Pugliese^{a,c}, R. Radogna^{a,b}, A. Ranieri^a, G. Selvaggi^{a,b}, L. Silvestris^{a,15}, R. Venditti^{a,b}

INFN Sezione di Bologna^a, Università di Bologna^b, Bologna, Italy

G. Abbiendi^a, C. Battilana¹⁵, D. Bonacorsi^{a,b}, S. Braibant-Giacomelli^{a,b}, L. Brigliadori^{a,b}, R. Campanini^{a,b}, P. Capiluppi^{a,b}, A. Castro^{a,b}, F. R. Cavallo^a, S. S. Chhibra^{a,b}, G. Codispoti^{a,b}, M. Cuffiani^{a,b}, G. M. Dallavalle^a, F. Fabbri^a, A. Fanfani^{a,b}, D. Fasanella^{a,b}, P. Giacomelli^a, C. Grandi^a, L. Guiducci^{a,b}, S. Marcellini^a, G. Masetti^a, A. Montanari^a, F. L. Navarria^{a,b}, A. Perrotta^a, A. M. Rossi^{a,b}, T. Rovelli^{a,b}, G. P. Siroli^{a,b}, N. Tosi^{a,b,15}

INFN Sezione di Catania^a, Università di Catania^b, Catania, Italy

G. Cappello^b, M. Chiorboli^{a,b}, S. Costa^{a,b}, A. Di Mattia^a, F. Giordano^{a,b}, R. Potenza^{a,b}, A. Tricomi^{a,b}, C. Tuve^{a,b}

INFN Sezione di Firenze^a, Università di Firenze^b, Firenze, Italy

G. Barbagli^a, V. Ciulli^{a,b}, C. Civinini^a, R. D'Alessandro^{a,b}, E. Focardi^{a,b}, V. Gori^{a,b}, P. Lenzi^{a,b}, M. Meschini^a, S. Paoletti^a, G. Sguazzoni^a, L. Viliani^{a,b,15}

INFN Laboratori Nazionali di Frascati, Frascati, Italy

L. Benussi, S. Bianco, F. Fabbri, D. Piccolo, F. Primavera¹⁵

INFN Sezione di Genova^a, Università di Genova^b, Genoa, Italy

V. Calvelli^{a,b}, F. Ferro^a, M. Lo Vetere^{a,b}, M. R. Monge^{a,b}, E. Robutti^a, S. Tosi^{a,b}

INFN Sezione di Milano-Bicocca^a, Università di Milano-Bicocca^b, Milan, Italy

L. Brianza, M. E. Dinardo^{a,b}, S. Fiorendi^{a,b}, S. Gennai^a, R. Gerosa^{a,b}, A. Ghezzi^{a,b}, P. Govoni^{a,b}, S. Malvezzi^a, R. A. Manzoni^{a,b,15}, B. Marzocchi^{a,b}, D. Menasce^a, L. Moroni^a, M. Paganoni^{a,b}, D. Pedrini^a, S. Pigazzini, S. Ragazzi^{a,b}, N. Redaelli^a, T. Tabarelli de Fatis^{a,b}

INFN Sezione di Napoli^a, Università di Napoli 'Federico II'^b, Napoli, Italy, Università della Basilicata^c, Potenza, Italy, Università G. Marconi^d, Rome, Italy

S. Buontempo^a, N. Cavallo^{a,c}, S. Di Guida^{a,d,15}, M. Esposito^{a,b}, F. Fabozzi^{a,c}, A. O. M. Iorio^{a,b}, G. Lanza^a, L. Lista^a, S. Meola^{a,d,15}, M. Merola^a, P. Paolucci^{a,15}, C. Sciacca^{a,b}, F. Thyssen

INFN Sezione di Padova^a, Università di Padova^b, Padova, Italy, Università di Trento^c, Trento, Italy

P. Azzi^{a,15}, N. Bacchetta^a, L. Benato^{a,b}, D. Bisello^{a,b}, A. Boletti^{a,b}, A. Branca^{a,b}, R. Carlin^{a,b}, P. Checchia^a, M. Dall'Osso^{a,b,15}, T. Dorigo^a, U. Dosselli^a, F. Gasparini^{a,b}, U. Gasparini^{a,b}, F. Gonella^a, A. Gozzelino^a, K. Kanishchev^{a,c}, S. Lacaprara^a, M. Margoni^{a,b}, A. T. Meneguzzo^{a,b}, J. Pazzini^{a,b,15}, N. Pozzobon^{a,b}, P. Ronchese^{a,b}, F. Simonetto^{a,b}, E. Torassa^a, M. Tosi^{a,b}, M. Zanetti, P. Zotto^{a,b}, A. Zucchetta^{a,b,15}, G. Zumerle^{a,b}

INFN Sezione di Pavia^a, Università di Pavia^b, Pavia, Italy

A. Braghieri^a, A. Magnani^{a,b}, P. Montagna^{a,b}, S. P. Ratti^{a,b}, V. Re^a, C. Riccardi^{a,b}, P. Salvini^a, I. Vai^{a,b}, P. Vitulo^{a,b}

INFN Sezione di Perugia^a, Università di Perugia^b, Perugia, Italy

L. Alunni Solestizi^{a,b}, G. M. Bilei^a, D. Ciangottini^{a,b}, L. Fanò^{a,b}, P. Lariccia^{a,b}, R. Leonardi^{a,b}, G. Mantovani^{a,b}, M. Menichelli^a, A. Saha^a, A. Santocchia^{a,b}

INFN Sezione di Pisa^a, Università di Pisa^b, Scuola Normale Superiore di Pisa^c, Pisa, Italy

K. Androsov^{a,31}, P. Azzurri^{a,15}, G. Bagliesi^a, J. Bernardini^a, T. Boccali^a, R. Castaldi^a, M. A. Ciocci^{a,31}, R. Dell'Orso^a, S. Donato^{a,c}, G. Fedì, L. Foà^{a,c,†}, A. Giassi^a, M. T. Grippo^{a,31}, F. Ligabue^{a,c}, T. Lomtadze^a, L. Martini^{a,b}, A. Messineo^{a,b}, F. Palla^a, A. Rizzi^{a,b}, A. Savoy-Navarro^{a,32}, P. Spagnolo^a, R. Tenchini^a, G. Tonelli^{a,b}, A. Venturi^a, P. G. Verdini^a

INFN Sezione di Roma^a, Università di Roma^b, Rome, Italy

L. Barone^{a,b}, F. Cavallari^a, G. D'imperio^{a,b,15}, D. Del Re^{a,b,15}, M. Diemoz^a, S. Gelli^{a,b}, C. Jorda^a, E. Longo^{a,b}, F. Margaroli^{a,b}, P. Meridiani^a, G. Organtini^{a,b}, R. Paramatti^a, F. Preiato^{a,b}, S. Rahatlou^{a,b}, C. Rovelli^a, F. Santanastasio^{a,b}

INFN Sezione di Torino^a, Università di Torino^b, Torino, Italy, Università del Piemonte Orientale^c, Novara, Italy

N. Amapane^{a,b}, R. Arcidiacono^{a,c,15}, S. Argiro^{a,b}, M. Arneodo^{a,c}, N. Bartosik^a, R. Bellan^{a,b}, C. Biino^a, N. Cartiglia^a, M. Costa^{a,b}, R. Covarelli^{a,b}, A. Degano^{a,b}, N. Demaria^a, L. Finco^{a,b}, B. Kiani^{a,b}, C. Mariotti^a, S. Maselli^a, E. Migliore^{a,b}, V. Monaco^{a,b}, E. Monteil^{a,b}, M. M. Obertino^{a,b}, L. Pacher^{a,b}, N. Pastrone^a, M. Pelliccioni^a, G. L. Pinna Angioni^{a,b}, F. Ravera^{a,b}, A. Romero^{a,b}, M. Ruspa^{a,c}, R. Sacchi^{a,b}, V. Sola^a, A. Solano^{a,b}, A. Staiano^a

INFN Sezione di Trieste^a, Università di Trieste^b, Trieste, Italy

S. Belforte^a, V. Candolise^{a,b}, M. Casarsa^a, F. Cossutti^a, G. Della Ricca^{a,b}, B. Gobbo^a, C. La Licata^{a,b}, A. Schizzi^{a,b}, A. Zanetti^a

Kangwon National University, Chunchon, Korea

S. K. Nam

Kyungpook National University, Daegu, Korea

D. H. Kim, G. N. Kim, M. S. Kim, D. J. Kong, S. Lee, S. W. Lee, Y. D. Oh, A. Sakharov, D. C. Son

Chonbuk National University, Jeonju, Korea

J. A. Brochero Cifuentes, H. Kim, T. J. Kim³³

Institute for Universe and Elementary Particles, Chonnam National University, Kwangju, Korea

S. Song

Korea University, Seoul, Korea

S. Cho, S. Choi, Y. Go, D. Gyun, B. Hong, Y. Kim, B. Lee, K. Lee, K. S. Lee, S. Lee, J. Lim, S. K. Park, Y. Roh

Seoul National University, Seoul, Korea

H. D. Yoo

University of Seoul, Seoul, Korea

M. Choi, H. Kim, H. Kim, J. H. Kim, J. S. H. Lee, I. C. Park, G. Ryu, M. S. Ryu

Sungkyunkwan University, Suwon, Korea

Y. Choi, J. Goh, D. Kim, E. Kwon, J. Lee, I. Yu

Vilnius University, Vilnius, Lithuania

V. Dudenas, A. Juodagalvis, J. Vaitkus

National Centre for Particle Physics, Universiti Malaya, Kuala Lumpur, MalaysiaI. Ahmed, Z. A. Ibrahim, J. R. Komaragiri, M. A. B. Md Ali³⁴, F. Mohamad Idris³⁵, W. A. T. Wan Abdullah, M. N. Yusli, Z. Zolkapli**Centro de Investigacion y de Estudios Avanzados del IPN, Mexico City, Mexico**E. Casimiro Linares, H. Castilla-Valdez, E. De La Cruz-Burelo, I. Heredia-De La Cruz³⁶, A. Hernandez-Almada, R. Lopez-Fernandez, J. Mejia Guisao, A. Sanchez-Hernandez**Universidad Iberoamericana, Mexico City, Mexico**

S. Carrillo Moreno, F. Vazquez Valencia

Benemerita Universidad Autonoma de Puebla, Puebla, Mexico

I. Pedraza, H. A. Salazar Ibarguen, C. Uribe Estrada

Universidad Autónoma de San Luis Potosí, San Luis Potosí, Mexico

A. Morelos Pineda

University of Auckland, Auckland, New Zealand

D. Krofcheck

University of Canterbury, Christchurch, New Zealand

P. H. Butler

National Centre for Physics, Quaid-I-Azam University, Islamabad, Pakistan

A. Ahmad, M. Ahmad, Q. Hassan, H. R. Hoorani, W. A. Khan, S. Qazi, M. Shoaib, M. Waqas

National Centre for Nuclear Research, Swierk, Poland

H. Bialkowska, M. Bluj, B. Boimska, T. Frueboes, M. Górski, M. Kazana, K. Nawrocki, K. Romanowska-Rybinska, M. Szleper, P. Traczyk, P. Zalewski

Institute of Experimental Physics, Faculty of Physics, University of Warsaw, Warsaw, PolandG. Brona, K. Bunkowski, A. Byszuk³⁷, K. Doroba, A. Kalinowski, M. Konecki, J. Krolikowski, M. Misiura, M. Olszewski, M. Walczak**Laboratório de Instrumentação e Física Experimental de Partículas, Lisbon, Portugal**

P. Bargassa, C. Beirão Da Cruz E Silva, A. Di Francesco, P. Faccioli, P. G. Ferreira Parracho, M. Gallinaro, J. Hollar, N. Leonardo, L. Lloret Iglesias, M. V. Nemallapudi, F. Nguyen, J. Rodrigues Antunes, J. Seixas, O. Toldaiev, D. Vadrucio, J. Varela, P. Vischia

Joint Institute for Nuclear Research, Dubna, RussiaI. Golutvin, A. Kamenev, V. Karjavin, V. Korenkov, G. Kozlov, A. Lanev, A. Malakhov, V. Matveev^{38,39}, V. V. Mitsyn, P. Moisenz, V. Palichik, V. Perelygin, S. Shmatov, S. Shulha, N. Skatchkov, V. Smirnov, E. Tikhonenko, N. Voytishin, A. Zarubin

Petersburg Nuclear Physics Institute, Gatchina, St. Petersburg, Russia

V. Golovtsov, Y. Ivanov, V. Kim⁴⁰, E. Kuznetsova⁴¹, P. Levchenko, V. Murzin, V. Oreshkin, I. Smirnov, V. Sulimov, L. Uvarov, S. Vavilov, A. Vorobyev

Institute for Nuclear Research, Moscow, Russia

Yu. Andreev, A. Dermenev, S. Gninenko, N. Golubev, A. Karneyeu, M. Kirsanov, N. Krasnikov, A. Pashenkov, D. Tlisov, A. Toropin

Institute for Theoretical and Experimental Physics, Moscow, Russia

V. Epshteyn, V. Gavrilov, N. Lychkovskaya, V. Popov, I. Pozdnyakov, G. Safronov, A. Spiridonov, M. Toms, E. Vlasov, A. Zhokin

National Research Nuclear University 'Moscow Engineering Physics Institute' (MEPhI), Moscow, Russia

M. Chadeeva, R. Chistov, M. Danilov, O. Markin, E. Tarkovskii

P.N. Lebedev Physical Institute, Moscow, Russia

V. Andreev, M. Azarkin³⁹, I. Dremin³⁹, M. Kirakosyan, A. Leonidov³⁹, G. Mesyats, S. V. Rusakov

Skobeltsyn Institute of Nuclear Physics, Lomonosov Moscow State University, Moscow, Russia

A. Baskakov, A. Belyaev, E. Boos, V. Bunichev, M. Dubinin⁴², L. Dudko, A. Gribushin, V. Klyukhin, O. Kodolova, I. Lokhtin, I. Miagkov, S. Obraztsov, S. Petrushanko, V. Savrin, A. Snigirev

Institute for High Energy Physics, State Research Center of Russian Federation, Protvino, Russia

I. Azhgirey, I. Bayshev, S. Bitiukov, V. Kachanov, A. Kalinin, D. Konstantinov, V. Krychkine, V. Petrov, R. Ryutin, A. Sobol, L. Tourtchanovitch, S. Troshin, N. Tyurin, A. Uzunian, A. Volkov

Faculty of Physics and Vinca Institute of Nuclear Sciences, University of Belgrade, Belgrade, Serbia

P. Adzic⁴³, P. Cirkovic, D. Devetak, J. Milosevic, V. Rekovic

Centro de Investigaciones Energéticas Medioambientales y Tecnológicas (CIEMAT), Madrid, Spain

J. Alcaraz Maestre, E. Calvo, M. Cerrada, M. Chamizo Llatas, N. Colino, B. De La Cruz, A. Delgado Peris, A. Escalante Del Valle, C. Fernandez Bedoya, J. P. Fernández Ramos, J. Flix, M. C. Fouz, P. Garcia-Abia, O. Gonzalez Lopez, S. Goy Lopez, J. M. Hernandez, M. I. Josa, E. Navarro De Martino, A. Pérez-Calero Yzquierdo, J. Puerta Pelayo, A. Quintario Olmeda, I. Redondo, L. Romero, M. S. Soares

Universidad Autónoma de Madrid, Madrid, Spain

J. F. de Trocóniz, M. Missiroli, D. Moran

Universidad de Oviedo, Oviedo, Spain

J. Cuevas, J. Fernandez Menendez, S. Folgueras, I. Gonzalez Caballero, E. Palencia Cortezon¹⁵, J. M. Vizan Garcia

Instituto de Física de Cantabria (IFCA), CSIC-Universidad de Cantabria, Santander, Spain

I. J. Cabrillo, A. Calderon, J. R. Castiñeiras De Saa, E. Curras, P. De Castro Manzano, M. Fernandez, J. Garcia-Ferrero, G. Gomez, A. Lopez Virto, J. Marco, R. Marco, C. Martinez Rivero, F. Matorras, J. Piedra Gomez, T. Rodrigo, A. Y. Rodríguez-Marrero, A. Ruiz-Jimeno, L. Scodellaro, N. Trevisani, I. Vila, R. Vilar Cortabitarte

CERN, European Organization for Nuclear Research, Geneva, Switzerland

D. Abbaneo, E. Auffray, G. Auzinger, M. Bachtis, P. Baillon, A. H. Ball, D. Barney, A. Benaglia, L. Benhabib, G. M. Berruti, P. Bloch, A. Bocci, A. Bonato, C. Botta, H. Breuker, T. Camporesi, R. Castello, M. Cepeda, G. Cerminara, M. D'Alfonso, D. d'Enterria, A. Dabrowski, V. Daponte, A. David, M. De Gruttola, F. De Guio, A. De Roeck, E. Di Marco⁴⁴, M. Dobson, M. Dordevic, B. Dorney, T. du Pree, D. Duggan, M. Dünser, N. Dupont, A. Elliott-Peisert, G. Franzoni, J. Fulcher, W. Funk, D. Gigi, K. Gill, M. Girone, F. Glege, R. Guida, S. Gundacker, M. Guthoff, J. Hammer, P. Harris, J. Hegeman, V. Innocente, P. Janot, H. Kirschenmann, V. Knünz, M. J. Kortelainen, K. Kousouris, P. Lecoq, C. Lourenço, M. T. Lucchini, N. Magini, L. Malgeri, M. Mannelli, A. Martelli, L. Masetti, F. Meijers, S. Mersi, E. Meschi, F. Moortgat, S. Morovic, M. Mulders, H. Neugebauer, S. Orfanelli⁴⁵, L. Orsini, L. Pape, E. Perez, M. Peruzzi, A. Petrilli, G. Petrucciani, A. Pfeiffer, M. Pierini, D. Piparo, A. Racz, T. Reis, G. Rolandi⁴⁶, M. Rovere, M. Ruan, H. Sakulin, J. B. Sauvan, C. Schäfer, C. Schwick, M. Seidel, A. Sharma, P. Silva, M. Simon, P. Sphicas⁴⁷, J. Steggemann, M. Stoye, Y. Takahashi, D. Treille, A. Triossi, A. Tsiros, V. Veckalns⁴⁸, G. I. Veres²², N. Wardle, H. K. Wöhri, A. Zagozdinska³⁷, W. D. Zeuner

Paul Scherrer Institut, Villigen, Switzerland

W. Bertl, K. Deiters, W. Erdmann, R. Horisberger, Q. Ingram, H. C. Kaestli, D. Kotlinski, U. Langenegger, T. Rohe

Institute for Particle Physics, ETH Zurich, Zurich, Switzerland

F. Bachmair, L. Bäni, L. Bianchini, B. Casal, G. Dissertori, M. Dittmar, M. Donegà, P. Eller, C. Grab, C. Heidegger, D. Hits, J. Hoss, G. Kasieczka, P. Lecomte[†], W. Lustermann, B. Mangano, M. Marionneau, P. Martinez Ruiz del Arbol, M. Masciovecchio, M. T. Meinhard, D. Meister, F. Micheli, P. Musella, F. Nessi-Tedaldi, F. Pandolfi, J. Pata, F. Pauss, G. Perrin, L. Perrozzi, M. Quittnat, M. Rossini, M. Schönenberger, A. Starodumov⁴⁹, M. Takahashi, V. R. Tavolaro, K. Theofilatos, R. Wallny

Universität Zürich, Zurich, Switzerland

T. K. Aarrestad, C. Amsler⁵⁰, L. Caminada, M. F. Canelli, V. Chiochia, A. De Cosa, C. Galloni, A. Hinzmann, T. Hreus, B. Kilminster, C. Lange, J. Ngadiuba, D. Pinna, G. Rauco, P. Robmann, D. Salerno, Y. Yang

National Central University, Chung-Li, Taiwan

K. H. Chen, T. H. Doan, Sh. Jain, R. Khurana, M. Konyushikhin, C. M. Kuo, W. Lin, Y. J. Lu, A. Pozdnyakov, S. S. Yu

National Taiwan University (NTU), Taipei, Taiwan

Arun Kumar, P. Chang, Y. H. Chang, Y. W. Chang, Y. Chao, K. F. Chen, P. H. Chen, C. Dietz, F. Fiori, U. Grundler, W.-S. Hou, Y. Hsiung, Y. F. Liu, R.-S. Lu, M. Miñano Moya, E. Petrakou, J. f. Tsai, Y. M. Tzeng

Faculty of Science, Department of Physics, Chulalongkorn University, Bangkok, Thailand

B. Asavapibhop, K. Kovitanggoon, G. Singh, N. Srimanobhas, N. Suwonjandee

Cukurova University, Adana, Turkey

A. Adiguzel, S. Cerci⁵¹, S. Damarseckin, Z. S. Demiroglu, C. Dozen, I. Dumanoglu, S. Girgis, G. Gokbulut, Y. Guler, E. Gurpinar, I. Hos, E. E. Kangal⁵², A. Kayis Topaksu, G. Onengut⁵³, K. Ozdemir⁵⁴, S. Ozturk⁵⁵, B. Tali⁵¹, H. Topakli⁵⁵, C. Zorbilmez

Physics Department, Middle East Technical University, Ankara, Turkey

B. Bilin, S. Bilmis, B. Isildak⁵⁶, G. Karapinar⁵⁷, M. Yalvac, M. Zeyrek

Bogazici University, Istanbul, Turkey

E. Gülmez, M. Kaya⁵⁸, O. Kaya⁵⁹, E. A. Yetkin⁶⁰, T. Yetkin⁶¹

Istanbul Technical University, Istanbul, Turkey

A. Cakir, K. Cankocak, S. Sen⁶²

Institute for Scintillation Materials of National Academy of Science of Ukraine, Kharkov, Ukraine

B. Grynyov

Kharkov Institute of Physics and Technology, National Scientific Center, Kharkov, Ukraine

L. Levchuk, P. Sorokin

University of Bristol, Bristol, UK

R. Aggleton, F. Ball, L. Beck, J. J. Brooke, D. Burns, E. Clement, D. Cussans, H. Flacher, J. Goldstein, M. Grimes, G. P. Heath, H. F. Heath, J. Jacob, L. Kreczko, C. Lucas, Z. Meng, D. M. Newbold⁶³, S. Paramesvaran, A. Poll, T. Sakuma, S. Seif El Nasr-storey, S. Senkin, D. Smith, V. J. Smith

Rutherford Appleton Laboratory, Didcot, UK

K. W. Bell, A. Belyaev⁶⁴, C. Brew, R. M. Brown, L. Calligaris, D. Cieri, D. J. A. Cockerill, J. A. Coughlan, K. Harder, S. Harper, E. Olaiya, D. Petyt, C. H. Shepherd-Themistocleous, A. Thea, I. R. Tomalin, T. Williams, S. D. Worm

Imperial College, London, UK

M. Baber, R. Bainbridge, O. Buchmuller, A. Bundock, D. Burton, S. Casasso, M. Citron, D. Colling, L. Corpe, P. Dauncey, G. Davies, A. De Wit, M. Della Negra, P. Dunne, A. Elwood, D. Futyan, Y. Haddad, G. Hall, G. Iles, R. Lane, R. Lucas⁶³, L. Lyons, A.-M. Magnan, S. Malik, L. Mastrolorenzo, J. Nash, A. Nikitenko⁴⁹, J. Pela, B. Penning, M. Pesaresi, D. M. Raymond, A. Richards, A. Rose, C. Seez, A. Tapper, K. Uchida, M. Vazquez Acosta⁶⁵, T. Virdee¹⁵, S. C. Zenz

Brunel University, Uxbridge, UK

J. E. Cole, P. R. Hobson, A. Khan, P. Kyberd, D. Leslie, I. D. Reid, P. Symonds, L. Teodorescu, M. Turner

Baylor University, Waco, USA

A. Borzou, K. Call, J. Dittmann, K. Hatakeyama, H. Liu, N. Pastika

The University of Alabama, Tuscaloosa, USA

O. Charaf, S. I. Cooper, C. Henderson, P. Rumerio

Boston University, Boston, USA

D. Arcaro, A. Avetisyan, T. Bose, D. Gastler, D. Rankin, C. Richardson, J. Rohlf, L. Sulak, D. Zou

Brown University, Providence, USA

J. Alimena, G. Benelli, E. Berry, D. Cutts, A. Ferapontov, A. Garabedian, J. Hakala, U. Heintz, O. Jesus, E. Laird, G. Landsberg, Z. Mao, M. Narain, S. Piperov, S. Sagir, R. Syarif

University of California, Davis, Davis, USA

R. Breedon, G. Breto, M. Calderon De La Barca Sanchez, S. Chauhan, M. Chertok, J. Conway, R. Conway, P. T. Cox, R. Erbacher, G. Funk, M. Gardner, W. Ko, R. Lander, C. Mclean, M. Mulhearn, D. Pellett, J. Pilot, F. Ricci-Tam, S. Shalhout, J. Smith, M. Squires, D. Stolp, M. Tripathi, S. Wilbur, R. Yohay

University of California, Los Angeles, USA

R. Cousins, P. Everaerts, A. Florent, J. Hauser, M. Ignatenko, D. Saltzberg, E. Takasugi, V. Valuev, M. Weber

University of California, Riverside, Riverside, USA

K. Burt, R. Clare, J. Ellison, J. W. Gary, G. Hanson, J. Heilman, M. Iova PANEVA, P. Jandir, E. Kennedy, F. Lacroix, O. R. Long, M. Malberti, M. Olmedo Negrete, A. Shrinivas, H. Wei, S. Wimpenny, B. R. Yates

University of California, San Diego, La Jolla, USA

J. G. Branson, G. B. Cerati, S. Cittolin, R. T. D'Agnolo, M. Derdzinski, A. Holzner, R. Kelley, D. Klein, J. Letts, I. Macneill, D. Olivito, S. Padhi, M. Pieri, M. Sani, V. Sharma, S. Simon, M. Tadel, A. Vartak, S. Wasserbaech⁶⁶, C. Welke, F. Würthwein, A. Yagil, G. Zevi Della Porta

University of California, Santa Barbara, Santa Barbara, USA

J. Bradmiller-Feld, C. Campagnari, A. Dishaw, V. Dutta, K. Flowers, M. Franco Sevilla, P. Geffert, C. George, F. Golf, L. Gouskos, J. Gran, J. Incandela, N. Mccoll, S. D. Mullin, J. Richman, D. Stuart, I. Suarez, C. West, J. Yoo

California Institute of Technology, Pasadena, USA

D. Anderson, A. Apresyan, J. Bendavid, A. Bornheim, J. Bunn, Y. Chen, J. Duarte, A. Mott, H. B. Newman, C. Pena, M. Spiropulu, J. R. Vlimant, S. Xie, R. Y. Zhu

Carnegie Mellon University, Pittsburgh, USA

M. B. Andrews, V. Azzolini, A. Calamba, B. Carlson, T. Ferguson, M. Paulini, J. Russ, M. Sun, H. Vogel, I. Vorobiev

University of Colorado Boulder, Boulder, USA

J. P. Cumalat, W. T. Ford, A. Gaz, F. Jensen, A. Johnson, M. Krohn, T. Mulholland, U. Nauenberg, K. Stenson, S. R. Wagner

Cornell University, Ithaca, USA

J. Alexander, A. Chatterjee, J. Chaves, J. Chu, S. Dittmer, N. Eggert, N. Mirman, G. Nicolas Kaufman, J. R. Patterson, A. Rinkevicius, A. Ryd, L. Skinnari, L. Soffi, W. Sun, S. M. Tan, W. D. Teo, J. Thom, J. Thompson, J. Tucker, Y. Weng, P. Wittich

Fermi National Accelerator Laboratory, Batavia, USA

S. Abdullin, M. Albrow, G. Apollinari, S. Banerjee, L. A. T. Bauerdick, A. Beretvas, J. Berryhill, P. C. Bhat, G. Bolla, K. Burkett, J. N. Butler, H. W. K. Cheung, F. Chlebana, S. Cihangir, V. D. Elvira, I. Fisk, J. Freeman, E. Gottschalk, L. Gray, D. Green, S. Grünendahl, O. Gutsche, J. Hanlon, D. Hare, R. M. Harris, S. Hasegawa, J. Hirschauer, Z. Hu, B. Jayatilaka, S. Jindariani, M. Johnson, U. Joshi, B. Klima, B. Kreis, S. Lammel, J. Lewis, J. Linacre, D. Lincoln, R. Lipton, T. Liu, R. Lopes De Sá, J. Lykken, K. Maeshima, J. M. Marraffino, S. Maruyama, D. Mason, P. McBride, P. Merkel, S. Mrenna, S. Nahn, C. Newman-Holmes[†], V. O'Dell, K. Pedro, O. Prokofyev, G. Rakness, E. Sexton-Kennedy, A. Soha, W. J. Spalding,

L. Spiegel, S. Stoynev, N. Strobbe, L. Taylor, S. Tkaczyk, N. V. Tran, L. Uplegger, E. W. Vaandering, C. Vernieri, M. Verzocchi, R. Vidal, M. Wang, H. A. Weber, A. Whitbeck

University of Florida, Gainesville, USA

D. Acosta, P. Avery, P. Bortignon, D. Bourilkov, A. Brinkerhoff, A. Carnes, M. Carver, D. Curry, S. Das, R. D. Field, I. K. Furic, J. Konigsberg, A. Korytov, K. Kotov, P. Ma, K. Matchev, H. Mei, P. Milenovic⁶⁷, G. Mitselmakher, D. Rank, R. Rossin, L. Shchutska, M. Snowball, D. Sperka, N. Terentyev, L. Thomas, J. Wang, S. Wang, J. Yelton

Florida International University, Miami, USA

S. Linn, P. Markowitz, G. Martinez, J. L. Rodriguez

Florida State University, Tallahassee, USA

A. Ackert, J. R. Adams, T. Adams, A. Askew, S. Bein, J. Bochenek, B. Diamond, J. Haas, S. Hagopian, V. Hagopian, K. F. Johnson, A. Khatiwada, H. Prosper, M. Weinberg

Florida Institute of Technology, Melbourne, USA

M. M. Baarmand, V. Bhopatkar, S. Colafranceschi⁶⁸, M. Hohlmann, H. Kalakhety, D. Noonan, T. Roy, F. Yumiceva

University of Illinois at Chicago (UIC), Chicago, USA

M. R. Adams, L. Apanasevich, D. Berry, R. R. Betts, I. Bucinskaite, R. Cavanaugh, O. Evdokimov, L. Gauthier, C. E. Gerber, D. J. Hofman, P. Kurt, C. O'Brien, I. D. Sandoval Gonzalez, P. Turner, N. Varelas, Z. Wu, M. Zakaria, J. Zhang

The University of Iowa, Iowa City, USA

B. Bilki⁶⁹, W. Clarida, K. Dilsiz, S. Durgut, R. P. Gandrajula, M. Haytmyradov, V. Khristenko, J.-P. Merlo, H. Mermerkaya⁷⁰, A. Mestvirishvili, A. Moeller, J. Nachtman, H. Ogul, Y. Onel, F. Ozok⁷¹, A. Penzo, C. Snyder, E. Tiras, J. Wetzel, K. Yi

Johns Hopkins University, Baltimore, USA

I. Anderson, B. A. Barnett, B. Blumenfeld, A. Cocoros, N. Eminizer, D. Fehling, L. Feng, A. V. Gritsan, P. Maksimovic, M. Osherson, J. Roskes, U. Sarica, M. Swartz, M. Xiao, Y. Xin, C. You

The University of Kansas, Lawrence, USA

P. Baringer, A. Bean, C. Bruner, J. Castle, R. P. Kenny III, A. Kropivnitskaya, D. Majumder, M. Malek, W. Mcbrayer, M. Murray, S. Sanders, R. Stringer, Q. Wang

Kansas State University, Manhattan, USA

A. Ivanov, K. Kaadze, S. Khalil, M. Makouski, Y. Maravin, A. Mohammadi, L. K. Saini, N. Skhirtladze, S. Toda

Lawrence Livermore National Laboratory, Livermore, USA

D. Lange, F. Rebassoo, D. Wright

University of Maryland, College Park, USA

C. Anelli, A. Baden, O. Baron, A. Belloni, B. Calvert, S. C. Eno, C. Ferraioli, J. A. Gomez, N. J. Hadley, S. Jabeen, R. G. Kellogg, T. Kolberg, J. Kunkle, Y. Lu, A. C. Mignerey, Y. H. Shin, A. Skuja, M. B. Tonjes, S. C. Tonwar

Massachusetts Institute of Technology, Cambridge, USA

A. Apyan, R. Barbieri, A. Baty, R. Bi, K. Bierwagen, S. Brandt, W. Busza, I. A. Cali, Z. Demiragli, L. Di Matteo, G. Gomez Ceballos, M. Goncharov, D. Gulhan, Y. Iiyama, G. M. Innocenti, M. Klute, D. Kovalskyi, K. Krajczar, Y. S. Lai, Y.-J. Lee, A. Levin, P. D. Luckey, A. C. Marini, C. McGinn, C. Mironov, S. Narayanan, X. Niu, C. Paus, C. Roland, G. Roland, J. Salfeld-Nebgen, G. S. F. Stephans, K. Sumorok, K. Tatar, M. Varma, D. Velicanu, J. Veverka, J. Wang, T. W. Wang, B. Wyslouch, M. Yang, V. Zhukova

University of Minnesota, Minneapolis, USA

A. C. Benvenuti, B. Dahmes, A. Evans, A. Finkel, A. Gude, P. Hansen, S. Kalafut, S. C. Kao, K. Klapoetke, Y. Kubota, Z. Lesko, J. Mans, S. Nourbakhsh, N. Ruckstuhl, R. Rusack, N. Tambe, J. Turkewitz

University of Mississippi, Oxford, USA

J. G. Acosta, S. Oliveros

University of Nebraska-Lincoln, Lincoln, USA

E. Avdeeva, R. Bartek, K. Bloom, S. Bose, D. R. Claes, A. Dominguez, C. Fangmeier, R. Gonzalez Suarez, R. Kamalieddin, D. Knowlton, I. Kravchenko, F. Meier, J. Monroy, F. Ratnikov, J. E. Siado, G. R. Snow, B. Stieger

State University of New York at Buffalo, Buffalo, USA

M. Alyari, J. Dolen, J. George, A. Godshalk, C. Harrington, I. Iashvili, J. Kaisen, A. Kharchilava, A. Kumar, A. Parker, S. Rappoccio, B. Roozbahani

Northeastern University, Boston, USA

G. Alverson, E. Barberis, D. Baumgartel, M. Chasco, A. Hortiangtham, A. Massironi, D. M. Morse, D. Nash, T. Orimoto, R. Teixeira De Lima, D. Trocino, R.-J. Wang, D. Wood, J. Zhang

Northwestern University, Evanston, USA

S. Bhattacharya, K. A. Hahn, A. Kubik, J. F. Low, N. Mucia, N. Odell, B. Pollack, M. H. Schmitt, K. Sung, M. Trovato, M. Velasco

University of Notre Dame, Notre Dame, USA

N. Dev, M. Hildreth, C. Jessop, D. J. Karmgard, N. Kellams, K. Lannon, N. Marinelli, F. Meng, C. Mueller, Y. Musienko³⁸, M. Planer, A. Reinsvold, R. Ruchti, N. Rupprecht, G. Smith, S. Taroni, N. Valls, M. Wayne, M. Wolf, A. Woodard

The Ohio State University, Columbus, USA

L. Antonelli, J. Brinson, B. Bylsma, L. S. Durkin, S. Flowers, A. Hart, C. Hill, R. Hughes, W. Ji, T. Y. Ling, B. Liu, W. Luo, D. Puigh, M. Rodenburg, B. L. Winer, H. W. Wulsin

Princeton University, Princeton, USA

O. Driga, P. Elmer, J. Hardenbrook, P. Hebda, S. A. Koay, P. Lujan, D. Marlow, T. Medvedeva, M. Mooney, J. Olsen, C. Palmer, P. Piroué, D. Stickland, C. Tully, A. Zuranski

University of Puerto Rico, Mayagüez, USA

S. Malik

Purdue University, West Lafayette, USA

A. Barker, V. E. Barnes, D. Benedetti, D. Bortoletto, L. Gutay, M. K. Jha, M. Jones, A. W. Jung, K. Jung, D. H. Miller, N. Neumeister, B. C. Radburn-Smith, X. Shi, I. Shipsey, D. Silvers, J. Sun, A. Svyatkovskiy, F. Wang, W. Xie, L. Xu

Purdue University Calumet, Hammond, USA

N. Parashar, J. Stupak

Rice University, Houston, USA

A. Adair, B. Akgun, Z. Chen, K. M. Ecklund, F. J. M. Geurts, M. Guilbaud, W. Li, B. Michlin, M. Northup, B. P. Padley, R. Redjimi, J. Roberts, J. Rorie, Z. Tu, J. Zabel

University of Rochester, Rochester, USA

B. Betchart, A. Bodek, P. de Barbaro, R. Demina, Y. Eshaq, T. Ferbel, M. Galanti, A. Garcia-Bellido, J. Han, O. Hindrichs, A. Khukhunaishvili, K. H. Lo, P. Tan, M. Verzetti

Rutgers, The State University of New Jersey, Piscataway, USA

J. P. Chou, E. Contreras-Campana, D. Ferencek, Y. Gershtein, E. Halkiadakis, M. Heindl, D. Hidas, E. Hughes, S. Kaplan, R. Kunnawalkam Elayavalli, A. Lath, K. Nash, H. Saka, S. Salur, S. Schnetzer, D. Sheffield, S. Somalwar, R. Stone, S. Thomas, P. Thomassen, M. Walker

University of Tennessee, Knoxville, USA

M. Foerster, J. Heideman, G. Riley, K. Rose, S. Spanier, K. Thapa

Texas A&M University, College Station, USA

O. Bouhali⁷², A. Castaneda Hernandez⁷², A. Celik, M. Dalchenko, M. De Mattia, A. Delgado, S. Dildick, R. Eusebi, J. Gilmore, T. Huang, T. Kamon⁷³, V. Krutelyov, R. Mueller, I. Osipenkov, Y. Pakhotin, R. Patel, A. Perloff, L. Perniè, D. Rathjens, A. Rose, A. Safonov, A. Tatarinov, K. A. Ulmer

Texas Tech University, Lubbock, USA

N. Akchurin, C. Cowden, J. Damgov, C. Dragoiu, P. R. Duerdo, J. Faulkner, S. Kunori, K. Lamichhane, S. W. Lee, T. Libeiro, S. Undleeb, I. Volobouev, Z. Wang

Vanderbilt University, Nashville, USA

E. Appelt, A. G. Delannoy, S. Greene, A. Gurrola, R. Janjam, W. Johns, C. Maguire, Y. Mao, A. Melo, H. Ni, P. Sheldon, S. Tuo, J. Velkovska, Q. Xu

University of Virginia, Charlottesville, USA

M. W. Arenton, P. Barria, B. Cox, B. Francis, J. Goodell, R. Hirosky, A. Ledovskoy, H. Li, C. Neu, T. Sinthuprasith, X. Sun, Y. Wang, E. Wolfe, J. Wood, F. Xia

Wayne State University, Detroit, USA

C. Clarke, R. Harr, P. E. Karchin, C. Kottachchi Kankanamge Don, P. Lamichhane, J. Sturdy

University of Wisconsin - Madison, Madison, WI, USA

D. A. Belknap, D. Carlsmith, S. Dasu, L. Dodd, S. Duric, B. Gomber, M. Grothe, M. Herndon, A. Hervé, P. Klabbers, A. Lanaro, A. Levine, K. Long, R. Loveless, A. Mohapatra, I. Ojalvo, T. Perry, G. A. Pierro, G. Polese, T. Ruggles, T. Sarangi, A. Savin, A. Sharma, N. Smith, W. H. Smith, D. Taylor, P. Verwilligen, N. Woods

† Deceased

- 1: Also at Vienna University of Technology, Vienna, Austria
- 2: Also at State Key Laboratory of Nuclear Physics and Technology, Peking University, Beijing, China
- 3: Also at Institut Pluridisciplinaire Hubert Curien, Université de Strasbourg, Université de Haute Alsace Mulhouse, CNRS/IN2P3, Strasbourg, France
- 4: Also at Universidade Estadual de Campinas, Campinas, Brazil
- 5: Also at Centre National de la Recherche Scientifique (CNRS) - IN2P3, Paris, France
- 6: Also at Université Libre de Bruxelles, Brussels, Belgium
- 7: Also at Laboratoire Leprince-Ringuet, Ecole Polytechnique, IN2P3-CNRS, Palaiseau, France
- 8: Also at Joint Institute for Nuclear Research, Dubna, Russia
- 9: Also at Helwan University, Cairo, Egypt
- 10: Now at Zewail City of Science and Technology, Zewail, Egypt
- 11: Also at Ain Shams University, Cairo, Egypt
- 12: Also at Fayoum University, El-Fayoum, Egypt
- 13: Now at British University in Egypt, Cairo, Egypt
- 14: Also at Université de Haute Alsace, Mulhouse, France
- 15: Also at CERN, European Organization for Nuclear Research, Geneva, Switzerland
- 16: Also at Skobeltsyn Institute of Nuclear Physics, Lomonosov Moscow State University, Moscow, Russia
- 17: Also at Tbilisi State University, Tbilisi, Georgia
- 18: Also at RWTH Aachen University, III. Physikalisches Institut A, Aachen, Germany
- 19: Also at University of Hamburg, Hamburg, Germany
- 20: Also at Brandenburg University of Technology, Cottbus, Germany
- 21: Also at Institute of Nuclear Research ATOMKI, Debrecen, Hungary
- 22: Also at MTA-ELTE Lendület CMS Particle and Nuclear Physics Group, Eötvös Loránd University, Budapest, Hungary
- 23: Also at University of Debrecen, Debrecen, Hungary
- 24: Also at Indian Institute of Science Education and Research, Bhopal, India
- 25: Also at University of Visva-Bharati, Santiniketan, India
- 26: Now at King Abdulaziz University, Jeddah, Saudi Arabia
- 27: Also at University of Ruhuna, Matara, Sri Lanka
- 28: Also at Isfahan University of Technology, Isfahan, Iran
- 29: Also at University of Tehran, Department of Engineering Science, Tehran, Iran
- 30: Also at Plasma Physics Research Center, Science and Research Branch, Islamic Azad University, Tehran, Iran
- 31: Also at Università degli Studi di Siena, Siena, Italy
- 32: Also at Purdue University, West Lafayette, USA
- 33: Now at Hanyang University, Seoul, Korea

- 34: Also at International Islamic University of Malaysia, Kuala Lumpur, Malaysia
- 35: Also at Malaysian Nuclear Agency, MOSTI, Kajang, Malaysia
- 36: Also at Consejo Nacional de Ciencia y Tecnología, Mexico city, Mexico
- 37: Also at Warsaw University of Technology, Institute of Electronic Systems, Warsaw, Poland
- 38: Also at Institute for Nuclear Research, Moscow, Russia
- 39: Now at National Research Nuclear University 'Moscow Engineering Physics Institute' (MEPhI), Moscow, Russia
- 40: Also at St. Petersburg State Polytechnical University, St. Petersburg, Russia
- 41: Also at University of Florida, Gainesville, USA
- 42: Also at California Institute of Technology, Pasadena, USA
- 43: Also at Faculty of Physics, University of Belgrade, Belgrade, Serbia
- 44: Also at INFN Sezione di Roma, Università di Roma, Rome, Italy
- 45: Also at National Technical University of Athens, Athens, Greece
- 46: Also at Scuola Normale e Sezione dell'INFN, Pisa, Italy
- 47: Also at National and Kapodistrian University of Athens, Athens, Greece
- 48: Also at Riga Technical University, Riga, Latvia
- 49: Also at Institute for Theoretical and Experimental Physics, Moscow, Russia
- 50: Also at Albert Einstein Center for Fundamental Physics, Bern, Switzerland
- 51: Also at Adiyaman University, Adiyaman, Turkey
- 52: Also at Mersin University, Mersin, Turkey
- 53: Also at Cag University, Mersin, Turkey
- 54: Also at Piri Reis University, Istanbul, Turkey
- 55: Also at Gaziosmanpasa University, Tokat, Turkey
- 56: Also at Ozyegin University, Istanbul, Turkey
- 57: Also at Izmir Institute of Technology, Izmir, Turkey
- 58: Also at Marmara University, Istanbul, Turkey
- 59: Also at Kafkas University, Kars, Turkey
- 60: Also at Istanbul Bilgi University, Istanbul, Turkey
- 61: Also at Yildiz Technical University, Istanbul, Turkey
- 62: Also at Hacettepe University, Ankara, Turkey
- 63: Also at Rutherford Appleton Laboratory, Didcot, UK
- 64: Also at School of Physics and Astronomy, University of Southampton, Southampton, UK
- 65: Also at Instituto de Astrofísica de Canarias, La Laguna, Spain
- 66: Also at Utah Valley University, Orem, USA
- 67: Also at University of Belgrade, Faculty of Physics and Vinca Institute of Nuclear Sciences, Belgrade, Serbia
- 68: Also at Facoltà Ingegneria, Università di Roma, Rome, Italy
- 69: Also at Argonne National Laboratory, Argonne, USA
- 70: Also at Erzincan University, Erzincan, Turkey
- 71: Also at Mimar Sinan University, Istanbul, Istanbul, Turkey
- 72: Also at Texas A&M University at Qatar, Doha, Qatar
- 73: Also at Kyungpook National University, Daegu, Korea